Supporting information

Synthesis and phase purity of the negative thermal expansion material ZrV_2O_7

[1,2]Aistė Miliūtė, [1]Joana Bustamante, [1,2]Stephanos Karafiludis, [1,2]Moritz Zöllner, [1]Mustapha Eddah, [1,2]Franziska Emmerling, [1]Björn Mieller*, [1,3]Janine George**, [1]Tomasz M. Stawski***
1 Federal Institute for Materials Research and Testing, Berlin, Germany.
2 Humboldt Universität zu Berlin, Department of Chemistry, Berlin, Germany.
3 Friedrich Schiller University of Jena, Institute of Solid-State Theory and Optics, Jena, Germany.
*bjoern.mieller@bam.de, **janine.george@bam.de, ***tomasz.stawski@bam.de

Table of Contents

Particle size distribution

Sample preparation

Ultrasonic sonotrode sonopuls HD 2200 with booster horn SH 213 and titanium sonotrode VS 70 T from Bandelin was used to disperse powders. Vanadium oxide and all mixed and ground powders were dispersed in 80 ml of ultrapure water (MiliQ, 18.2 MΩ·cm at 25 °C). The zirconium oxide powder was dispersed in 80 ml 3 mmol/L sodium tetraphosphate solution.

The suspension was sonicated with pulsed ultrasound (50%/50%) at approx. 80% of the maximum power in staggered ultrasound times (initially for one minute, followed by two-minute steps), each of which was followed by a measurement.

Measurement procedure

3-6 mL of the pre-dispersed suspensions were agitated at a stirring and pumping maximum speed of 3500 rpm. The scattered light data was recorded for 10 s for each wavelength (red laser - 633 nm and blue diode - 470 nm). One measurement consisted of 5 averaged individual data collections. The background of a corresponding particle-free dispersing liquid was determined before each measurement.

After recording the scattered light data, the particle size distribution was calculated. For the zirconium oxide, the evaluation was carried out using Mie-theory, considering the complex refractive index (real part n and imaginary part k) of the sample and fluid. The following complex refractive index data were used:

n_{red} (ZrO_2) = 2.152 n_{blue} (ZrO_2) = 2.189 n (fluid) = 1.33

k_{red} (ZrO_2) = 0.05 k_{blue} (ZrO_2) = 0.02

The measurements of vanadium oxide and all mixtures were evaluated using the Fraunhofer approximation, as the refractive index was either unknown or could not be specified.

Table S1. Summary and results of the particle size distribution analysis.

R-Nr	Sample Description	$d_{10.3}$, (µm)	$d_{50.3}$, (µm)	$d_{90.3}$, (µm)	$d_{97.3}$, (µm)	Liquid	Model	US	US- %
48	Zirconium(IV)-oxide, commercial powder, Art.-Nr. 9303.1, 0.5 kg, Ch: 102321171, Carl Roth	0.70	1.81	5.90	9.8	3 mmol/L $Na_4P_2O_7$	Mie	5’	80%, 50/50
186	Vanadium(V)-oxide, commercial powder, Art.-Nr. 008133, 0.5 kg, Ch: 120121, Chempur	0.56	1.41	3.71	4.8	Water	Fh	13‘	80%, 50/50
174	ZrO_2 + V_2O_5, planetary mill, 10 min	0.50	1.24	3.42	4.6	Water	Fh	7'	80%, 50/50
210	ZrO_2 + V_2O_5, planetary mill, 40 min	0.47	1.22	4.01	5.8	Water	Fh	5'	80%, 50/50
192	ZrO_2 + V_2O_5, planetary mill, 90 min	0.42	1.01	2.66	3.6	Water	Fh	5'	80%, 50/50
228	ZrO_2 + V_2O_5, planetary mill, 120 min	0.41	0.97	2.56	3.5	Water	Fh	5’	80%, 50/50
252	ZrO_2 + V_2O_5, planetary mill, 180 min	0.38	0.91	2.36	3.2	Water	Fh	5’	80%, 50/50

X-ray diffraction (XRD)

X-ray powder diffraction (Debye-Scherrer transmission geometry)

This method was used to collect diffraction patterns of sol-gel_100 °C and sol-gel_160 °C. XRD data was collected on a D8 Discover (Bruker, AXS, Germany) with Cu K_α (1.54184 Å) radiation monochromatised via a Johansson monochromator. A Lynxeye XE Silicon strip detector was used for data acquisition in transmission geometry. The sample was loaded into a quartz capillary with an internal diameter of 1.0 mm. Diffraction data were collected at room temperature over a *q* range from 0.356 to 5.243 $Å^{-1}$ with a step size of 0.009° and a step time of 7 s. The total time per measurement was 16 hours. This relatively long measurement time is typical for measurements in transmission geometry.

X-ray powder diffraction (Bragg-Brentano reflection geometry)

This method was used to collect diffraction patterns for all solid-state reactions and sol-gel_RO^-, sol-gel_Cl, and solvothermal reaction products. Data was recorded with a D8 Advance diffractometer (Bruker AXS, Karlsruhe, Germany) equipped with an energy-dispersive LynxEye XE-T detector. The powder specimens were prepared in zero background sample holders. Measurements were performed with a copper X-ray source with a Cu K_α wavelength of 1.54184 Å without a monochromator. The measurements were conducted in Bragg-Brentano geometry and an X-ray tube power of 40 kV, 40 mA. The selected parameters were as follows: 0.356 - 6.25 $Å^{-1}$ measurement range in a *q* scale, 0.01° step size, 1.15 s measurement time per step and 3 h total measurement time. The total time per measurement was 3 hours.

Synchrotron experiments

High-quality XRD data of the sol-gel_RO^- synthesis product was collected in DESY PETRA III P02.1 Powder Diffraction and Total Scattering Beamline with fixed 60 keV energy (λ ~0.207 Å). A Perkin Elmer XRD1621 area detector mounted on a long translation stage was used. Powders were loaded into a quartz capillary with an internal diameter of 1.0 mm. Diffraction data were collected at room temperature over a *q* range from 0.0015 to 5.47 $Å^{-1}$.

Phase quantification

Phase quantification was performed using Rietveld refinement with Match! software that uses the FullProf program[1,2]. Diffraction patterns in the range from 1.065 to 4.966 $Å^{-1}$ were used for refinements. The experimental pattern, Rietveld refinement, peak positions and difference plot are provided together with parameters used in Rietveld refinement.

Phase Analysis Report.
Sample: solid-state 40’ 5h

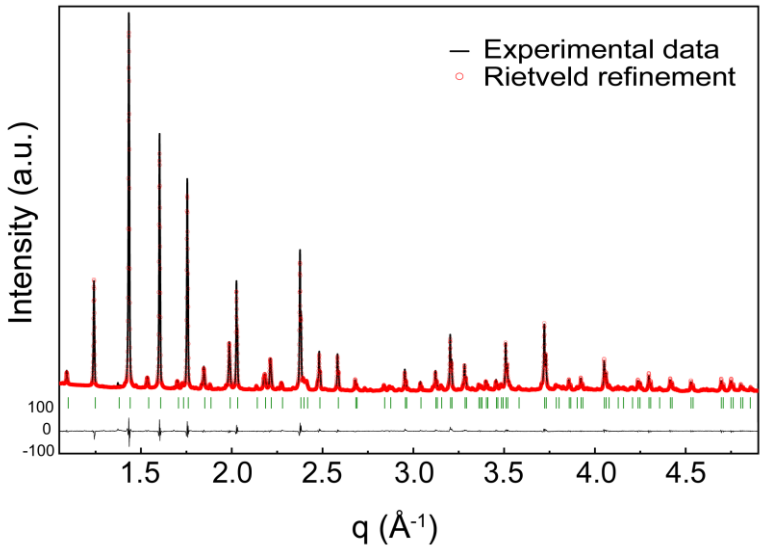

Figure S1. Rietveld refinement plot, showing the observed (black), calculated (red) and difference patterns of ZrV_2O_7 solid-state 40’ 5h sample. Vertical lines indicate the positions of the Bragg reflections.

Sample and refinement data

Data range	13.908° - 75.055° 2Θ
Original data range	5.000° - 99.985°
Step size	0.010
Rietveld refinement converged	Yes
α2 subtracted	No
Background subtracted	No
Data smoothed	No
Specimen displacement correction (Bragg-Brentano geometry)	T = (-s/R) = 0.00084333
Radiation	X-rays
Method	Rietveld refinement
Automatic refinement	No
Final weighted average Bragg R factor	4.3
Final reduced chi^2	8.8

Matched phases

Amount (%)	Name	Formula sum	COD ID
72.9		O7 V2 Zr	2002983
15.6	Shcherbinaite	O5 V2	9012221
11.5	Baddeleyite	O2 Zr	9007485
3.5	Unidentified peak area		

Parameter List for Refinement

Parameter	Final value	Parameter	Final value	Parameter	Final value
SyCos_pat1	0.0966386	Occ_V16_ph1	1.01494	Occ_O41_ph1	1
Bck_0_pat1	0.983263	X_V17_ph1	0.12459	X_O42_ph1	0.26222
Scale_ph1_pat1	8.88784E-07	Y_V17_ph1	0.12459	Y_O42_ph1	0.1951
Cell_A_ph1_pat1	26.3207	Z_V17_ph1	0.12459	Z_O42_ph1	0.18376
Scale_ph2_pat1	0.00167417	Biso_V17_ph1	0.734	Biso_O42_ph1	1.958
Cell_A_ph2_pat1	11.5167	Occ_V17_ph1	0.930779	Occ_O42_ph1	1
Cell_B_ph2_pat1	3.5635	X_O18_ph1	0.48004	X_O43_ph1	0.59815
Cell_C_ph2_pat1	4.38044	Y_O18_ph1	0.06539	Y_O43_ph1	-0.01624
Scale_ph3_pat1	0.00116156	Z_O18_ph1	0.1262	Z_O43_ph1	0.03707
Cell_A_ph3_pat1	5.14837	Biso_O18_ph1	1.523	Biso_O43_ph1	1.531
Cell_B_ph3_pat1	5.20688	Occ_O18_ph1	1	Occ_O43_ph1	1
Cell_C_ph3_pat1	5.31962	X_O19_ph1	0.40009	X_O44_ph1	0.06452
Cell_E_ph3_pat1	99.2169	Y_O19_ph1	0.12892	Y_O44_ph1	0.14578
Zero_pat1	0	Z_O19_ph1	0.1466	Z_O44_ph1	0.12622
SySin_pat1	0	Biso_O19_ph1	1.871	Biso_O44_ph1	1.713
Lambda_pat1	1.54187	Occ_O19_ph1	1	Occ_O44_ph1	1
P0_mabs_pat1	0	X_O20_ph1	0.47258	X_O45_ph1	0.4973
Cp_mabs_pat1	0	Y_O20_ph1	0.15725	Y_O45_ph1	0.155
Tau_mabs_pat1	0.1	Z_O20_ph1	0.07648	Z_O45_ph1	0.1807
Bck_1_pat1	1.73755	Biso_O20_ph1	1.555	Biso_O45_ph1	2.423
Bck_2_pat1	0.000379844	Occ_O20_ph1	1	Occ_O45_ph1	1
Bck_3_pat1	-0.0167517	X_O21_ph1	0.49048	X_O46_ph1	0.5101
Bover_ph1_pat1	0	Y_O21_ph1	0.39627	Y_O46_ph1	0.492
Strain1_ph1_pat1	0	Z_O21_ph1	0.12804	Z_O46_ph1	0.1707
Strain2_ph1_pat1	0	Biso_O21_ph1	1.618	Biso_O46_ph1	2.55
Strain3_ph1_pat1	0	Occ_O21_ph1	1	Occ_O46_ph1	1
G-Size_ph1_pat1	0	X_O22_ph1	0.4726	X_O47_ph1	0.3362
L-Size_ph1_pat1	0	Y_O22_ph1	0.48128	Y_O47_ph1	0.3271
Y-cos_ph1_pat1	0	Z_O22_ph1	0.07129	Z_O47_ph1	0.173
EtaRght0_ph1_pat1	0	Biso_O22_ph1	1.823	Biso_O47_ph1	2.866
X-tan_ph1_pat1	0.0174632	Occ_O22_ph1	1	Occ_O47_ph1	1
U-Cagl_ph1_pat1	0	X_O23_ph1	0.41032	X_O48_ph1	0.3357
V-Cagl_ph1_pat1	0	Y_O23_ph1	0.45904	Y_O48_ph1	0.1759
W-Cagl_ph1_pat1	0.00657514	Z_O23_ph1	0.15181	Z_O48_ph1	0.0004
EtaPV_ph1_pat1	0.0434719	Biso_O23_ph1	1.594	Biso_O48_ph1	2.645
Cell_B_ph1_pat1	26.3207	Occ_O23_ph1	1	Occ_O48_ph1	1
Cell_C_ph1_pat1	26.3207	X_O24_ph1	0.3524	X_O49_ph1	0.16284
Cell_D_ph1_pat1	90	Y_O24_ph1	0.3083	Y_O49_ph1	0.16284
Cell_E_ph1_pat1	90	Z_O24_ph1	0.06917	Z_O49_ph1	0.16284
Cell_F_ph1_pat1	90	Biso_O24_ph1	2.044	Biso_O49_ph1	2.842
Or1_ph1_pat1	-0.0216295	Occ_O24_ph1	1	Occ_O49_ph1	1
Or2_ph1_pat1	0	X_O25_ph1	0.3565	X_O50_ph1	0.5
Asym1_ph1_pat1	0	Y_O25_ph1	0.22994	Y_O50_ph1	0.5
Asym2_ph1_pat1	0.0238548	Z_O25_ph1	0.1359	Z_O50_ph1	0.5
Asym3_ph1_pat1	0	Biso_O25_ph1	2.218	Biso_O50_ph1	2.85
Asym4_ph1_pat1	0	Occ_O25_ph1	1	Occ_O50_ph1	1
X_Zr1_ph1	0.497434	X_O26_ph1	0.43193	Bover_ph2_pat1	0

Y_Zr1_ph1	-0.001114	Y_O26_ph1	0.3013	Strain1_ph2_pat1	0
Z_Zr1_ph1	0.165602	Z_O26_ph1	0.13571	Strain2_ph2_pat1	0
Biso_Zr1_ph1	0.497	Biso_O26_ph1	1.91	Strain3_ph2_pat1	0
Occ_Zr1_ph1	0.960707	Occ_O26_ph1	1	G-Size_ph2_pat1	0
X_Zr2_ph1	0.500084	X_O27_ph1	0.23557	L-Size_ph2_pat1	0
Y_Zr2_ph1	0.32661	Y_O27_ph1	0.3606	Y-cos_ph2_pat1	0
Z_Zr2_ph1	0.164329	Z_O27_ph1	0.18436	EtaRght0_ph2_pat1	0
Biso_Zr2_ph1	0.481	Biso_O27_ph1	1.879	X-tan_ph2_pat1	0.0184458
Occ_Zr2_ph1	1.10172	Occ_O27_ph1	1	U-Cagl_ph2_pat1	0
X_Zr3_ph1	0.496217	X_O28_ph1	0.3133	V-Cagl_ph2_pat1	0
Y_Zr3_ph1	0.170143	Y_O28_ph1	0.42848	W-Cagl_ph2_pat1	0.0125547
Z_Zr3_ph1	0.34384	Z_O28_ph1	0.1951	EtaPV_ph2_pat1	0.138715
Biso_Zr3_ph1	0.426	Biso_O28_ph1	2.029	Cell_D_ph2_pat1	90
Occ_Zr3_ph1	0.960551	Occ_O28_ph1	1	Cell_E_ph2_pat1	90
X_Zr4_ph1	0.331355	X_O29_ph1	0.29834	Cell_F_ph2_pat1	90
Y_Zr4_ph1	0.162024	Y_O29_ph1	0.35604	Or1_ph2_pat1	0
Z_Zr4_ph1	0.166102	Z_O29_ph1	0.26787	Or2_ph2_pat1	0
Biso_Zr4_ph1	0.505	Biso_O29_ph1	1.831	Asym1_ph2_pat1	0
Occ_Zr4_ph1	0.998362	Occ_O29_ph1	1	Asym2_ph2_pat1	0
X_Zr5_ph1	0.334645	X_O30_ph1	0.3018	Asym3_ph2_pat1	0
Y_Zr5_ph1	0.334645	Y_O30_ph1	0.14271	Asym4_ph2_pat1	0
Z_Zr5_ph1	0.334645	Z_O30_ph1	0.09573	X_V1_ph2	0.60299
Biso_Zr5_ph1	0.536	Biso_O30_ph1	1.792	Y_V1_ph2	0.25
Occ_Zr5_ph1	0.928984	Occ_O30_ph1	1	Z_V1_ph2	0.10574
X_Zr6_ph1	0	X_O31_ph1	0.24174	Biso_V1_ph2	1.4285
Y_Zr6_ph1	0	Y_O31_ph1	0.12759	Occ_V1_ph2	0.980082
Z_Zr6_ph1	0	Z_O31_ph1	0.01154	X_O2_ph2	0.42586
Biso_Zr6_ph1	0.505	Biso_O31_ph1	1.65	Y_O2_ph2	0.25
Occ_Zr6_ph1	0.847517	Occ_O31_ph1	1	Z_O2_ph2	-0.00275127
X_V7_ph1	0.46207	X_O32_ph1	0.32893	Biso_O2_ph2	1.3319
Y_V7_ph1	0.12653	Y_O32_ph1	0.07216	Occ_O2_ph2	1.06267
Z_V7_ph1	0.13145	Z_O32_ph1	0.02455	X_O3_ph2	0.6046
Biso_V7_ph1	0.781	Biso_O32_ph1	1.689	Y_O3_ph2	0.25
Occ_V7_ph1	1.0171	Occ_O32_ph1	1	Z_O3_ph2	0.4572
X_V8_ph1	0.4703	X_O33_ph1	0.35597	Biso_O3_ph2	1.3902
Y_V8_ph1	0.45683	Y_O33_ph1	0.27237	Occ_O3_ph2	1.09045
Z_V8_ph1	0.12993	Z_O33_ph1	-0.03702	X_O4_ph2	0.25
Biso_V8_ph1	0.742	Biso_O33_ph1	1.587	Y_O4_ph2	0.75
Occ_V8_ph1	0.92225	Occ_O33_ph1	1	Z_O4_ph2	0.0008
X_V9_ph1	0.36952	X_O34_ph1	0.43498	Biso_O4_ph2	1.6936
Y_V9_ph1	0.29152	Y_O34_ph1	0.20653	Occ_O4_ph2	1.03565
Z_V9_ph1	0.12774	Z_O34_ph1	-0.01851	Bover_ph3_pat1	0
Biso_V9_ph1	0.742	Biso_O34_ph1	1.721	Strain1_ph3_pat1	0
Occ_V9_ph1	1.03972	Occ_O34_ph1	1	Strain2_ph3_pat1	0

X_V10_ph1	0.29521	X_O35_ph1	0.37015	Strain3_ph3_pat1	0
Y_V10_ph1	0.36857	Y_O35_ph1	0.18931	G-Size_ph3_pat1	0
Z_V10_ph1	0.20539	Z_O35_ph1	-0.09934	L-Size_ph3_pat1	0
Biso_V10_ph1	0.757	Biso_O35_ph1	1.808	Y-cos_ph3_pat1	0
Occ_V10_ph1	1.03663	Occ_O35_ph1	1	EtaRght0_ph3_pat1	0
X_V11_ph1	0.30164	X_O36_ph1	0.5206	X-tan_ph3_pat1	0.00575546
Y_V11_ph1	0.12878	Y_O36_ph1	0.53508	U-Cagl_ph3_pat1	0
Z_V11_ph1	0.03361	Z_O36_ph1	0.26734	V-Cagl_ph3_pat1	0
Biso_V11_ph1	0.679	Biso_O36_ph1	1.744	W-Cagl_ph3_pat1	0.0114984
Occ_V11_ph1	1.04149	Occ_O36_ph1	1	EtaPV_ph3_pat1	0.381377
X_V12_ph1	0.37478	X_O37_ph1	0.51715	Cell_D_ph3_pat1	90
Y_V12_ph1	0.21139	Y_O37_ph1	0.59745	Cell_F_ph3_pat1	90
Z_V12_ph1	-0.0395	Z_O37_ph1	0.18395	Or1_ph3_pat1	0
Biso_V12_ph1	0.765	Biso_O37_ph1	1.871	Or2_ph3_pat1	0
Occ_V12_ph1	0.933972	Occ_O37_ph1	1	Asym1_ph3_pat1	0
X_V13_ph1	0.53727	X_O38_ph1	0.60074	Asym2_ph3_pat1	0
Y_V13_ph1	0.54143	Y_O38_ph1	0.53739	Asym3_ph3_pat1	0
Z_V13_ph1	0.20594	Z_O38_ph1	0.20051	Asym4_ph3_pat1	0
Biso_V13_ph1	0.757	Biso_O38_ph1	1.808	X_Zr1_ph3	0.27882
Occ_V13_ph1	1.0105	Occ_O38_ph1	1	Y_Zr1_ph3	0.040319
X_V14_ph1	0.53403	X_O39_ph1	0.51072	Z_Zr1_ph3	0.20967
Y_V14_ph1	0.20035	Y_O39_ph1	0.25854	Biso_Zr1_ph3	1.4753
Z_V14_ph1	0.21313	Z_O39_ph1	0.20207	Occ_Zr1_ph3	0.995115
Biso_V14_ph1	0.726	Biso_O39_ph1	1.823	X_O2_ph3	0.061764
Occ_V14_ph1	0.994503	Occ_O39_ph1	1	Y_O2_ph3	0.33566
X_V15_ph1	0.20147	X_O40_ph1	0.59407	Z_O2_ph3	0.34319
Y_V15_ph1	0.20147	Y_O40_ph1	0.19718	Biso_O2_ph3	0.54183
Z_V15_ph1	0.20147	Z_O40_ph1	0.19242	Occ_O2_ph3	1.0264
Biso_V15_ph1	0.813	Biso_O40_ph1	1.808	X_O3_ph3	0.44045
Occ_V15_ph1	0.940115	Occ_O40_ph1	1	Y_O3_ph3	0.75931
X_V16_ph1	0.53834	X_O41_ph1	0.5323	Z_O3_ph3	0.47982
Y_V16_ph1	0.53834	Y_O41_ph1	0.18804	Biso_O3_ph3	0.10994
Z_V16_ph1	0.53834	Z_O41_ph1	0.2758	Occ_O3_ph3	1.01494
Biso_V16_ph1	0.686	Biso_O41_ph1	1.847		

Phase Analysis Report.
Commercially available ZrV_2O_7

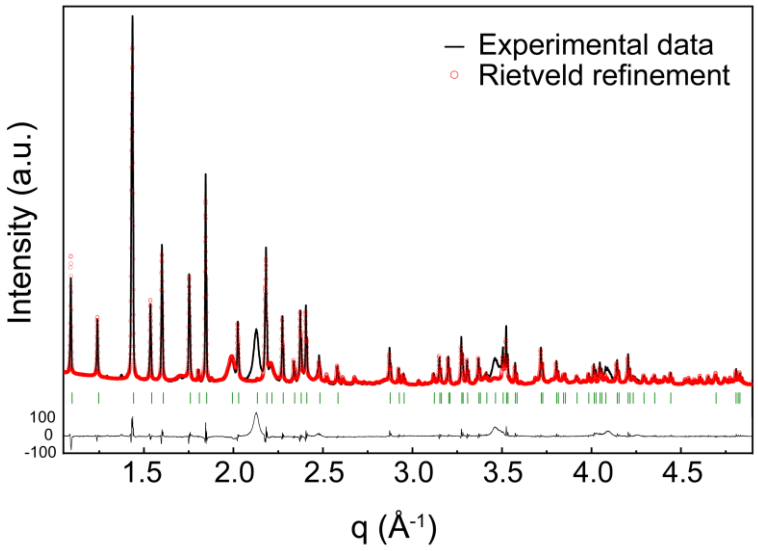

Figure S2. Rietveld refinement plot, showing the observed (black), calculated (red) and difference patterns of commercially available ZrV_2O_7. Vertical lines indicate the positions of the Bragg reflections.

Sample and refinement data

Data range	14.315° - 77.087° 2Θ
Original data range	5.000° - 99.985°
Step size	0.010
Rietveld refinement converged	Yes
α2 subtracted	No
Background subtracted	No
Data smoothed	No
Specimen displacement correction (Bragg-Brentano geometry)	T = (-s/R) = 0.0011664
Radiation	X-rays
Method	Rietveld refinement
Automatic refinement	No
Final weighted average Bragg R factor	17.0
Final reduced chi^2	77.1

Matched phases

Amount (%)	Name	Formula sum	COD ID
26.5		O7 V2 Zr	2002983
56.6	Shcherbinaite	O5 V2	9012221
16.9	Baddeleyite	O2 Zr	9007485
11.2	Unidentified peak area		

Parameter List for Refinement

Parameter	Final value	Parameter	Final value	Parameter	Final value
SyCos_pat1	0.133662	Y_V9_ph2	0.29152	Y_O34_ph2	0.20653
Scale_ph1_pat1	0.00613601	Z_V9_ph2	0.12774	Z_O34_ph2	-0.01851
Cell_A_ph1_pat1	11.5131	Biso_V9_ph2	0.742	Biso_O34_ph2	1.721
Cell_B_ph1_pat1	3.56428	Occ_V9_ph2	1	Occ_O34_ph2	1
Cell_C_ph1_pat1	4.37331	X_V10_ph2	0.29521	X_O35_ph2	0.37015
Asym2_ph1_pat1	0.0159459	Y_V10_ph2	0.36857	Y_O35_ph2	0.18931
Scale_ph2_pat1	3.11875E-07	Z_V10_ph2	0.20539	Z_O35_ph2	-0.09934
Scale_ph3_pat1	0.00172638	Biso_V10_ph2	0.757	Biso_O35_ph2	1.808
Zero_pat1	0	Occ_V10_ph2	1	Occ_O35_ph2	1
SySin_pat1	0	X_V11_ph2	0.30164	X_O36_ph2	0.5206
Lambda_pat1	1.54187	Y_V11_ph2	0.12878	Y_O36_ph2	0.53508
P0_mabs_pat1	0	Z_V11_ph2	0.03361	Z_O36_ph2	0.26734
Cp_mabs_pat1	0	Biso_V11_ph2	0.679	Biso_O36_ph2	1.744
Tau_mabs_pat1	0.1	Occ_V11_ph2	1	Occ_O36_ph2	1
Bck_0_pat1	0.966494	X_V12_ph2	0.37478	X_O37_ph2	0.51715
Bck_1_pat1	6.61292	Y_V12_ph2	0.21139	Y_O37_ph2	0.59745
Bck_2_pat1	-0.0188351	Z_V12_ph2	-0.0395	Z_O37_ph2	0.18395
Bck_3_pat1	0	Biso_V12_ph2	0.765	Biso_O37_ph2	1.871
Bover_ph1_pat1	0	Occ_V12_ph2	1	Occ_O37_ph2	1
Strain1_ph1_pat1	0	X_V13_ph2	0.53727	X_O38_ph2	0.60074
Strain2_ph1_pat1	0	Y_V13_ph2	0.54143	Y_O38_ph2	0.53739
Strain3_ph1_pat1	0	Z_V13_ph2	0.20594	Z_O38_ph2	0.20051
G-Size_ph1_pat1	0	Biso_V13_ph2	0.757	Biso_O38_ph2	1.808
L-Size_ph1_pat1	0	Occ_V13_ph2	1	Occ_O38_ph2	1
Y-cos_ph1_pat1	0	X_V14_ph2	0.53403	X_O39_ph2	0.51072
EtaRght0_ph1_pat1	0	Y_V14_ph2	0.20035	Y_O39_ph2	0.25854
X-tan_ph1_pat1	0.0134638	Z_V14_ph2	0.21313	Z_O39_ph2	0.20207
U-Cagl_ph1_pat1	0	Biso_V14_ph2	0.726	Biso_O39_ph2	1.823
V-Cagl_ph1_pat1	0	Occ_V14_ph2	1	Occ_O39_ph2	1
W-Cagl_ph1_pat1	0.00586025	X_V15_ph2	0.20147	X_O40_ph2	0.59407
EtaPV_ph1_pat1	0.308864	Y_V15_ph2	0.20147	Y_O40_ph2	0.19718
Cell_D_ph1_pat1	90	Z_V15_ph2	0.20147	Z_O40_ph2	0.19242
Cell_E_ph1_pat1	90	Biso_V15_ph2	0.813	Biso_O40_ph2	1.808
Cell_F_ph1_pat1	90	Occ_V15_ph2	1	Occ_O40_ph2	1
Or1_ph1_pat1	0	X_V16_ph2	0.53834	X_O41_ph2	0.5323
Or2_ph1_pat1	0	Y_V16_ph2	0.53834	Y_O41_ph2	0.18804
Asym1_ph1_pat1	0	Z_V16_ph2	0.53834	Z_O41_ph2	0.2758
Asym3_ph1_pat1	0	Biso_V16_ph2	0.686	Biso_O41_ph2	1.847
Asym4_ph1_pat1	0	Occ_V16_ph2	1	Occ_O41_ph2	1
X_V1_ph1	0.60123	X_V17_ph2	0.12459	X_O42_ph2	0.26222
Y_V1_ph1	0.25	Y_V17_ph2	0.12459	Y_O42_ph2	0.1951
Z_V1_ph1	0.1086	Z_V17_ph2	0.12459	Z_O42_ph2	0.18376
Biso_V1_ph1	0.592	Biso_V17_ph2	0.734	Biso_O42_ph2	1.958
Occ_V1_ph1	1	Occ_V17_ph2	1	Occ_O42_ph2	1
X_O2_ph1	0.4309	X_O18_ph2	0.48004	X_O43_ph2	0.59815
Y_O2_ph1	0.25	Y_O18_ph2	0.06539	Y_O43_ph2	-0.01624

Z_O2_ph1	-0.0028	Z_O18_ph2	0.1262	Z_O43_ph2	0.03707
Biso_O2_ph1	0.781	Biso_O18_ph2	1.523	Biso_O43_ph2	1.531
Occ_O2_ph1	1	Occ_O18_ph2	1	Occ_O43_ph2	1
X_O3_ph1	0.6045	X_O19_ph2	0.40009	X_O44_ph2	0.06452
Y_O3_ph1	0.25	Y_O19_ph2	0.12892	Y_O44_ph2	0.14578
Z_O3_ph1	0.4697	Z_O19_ph2	0.1466	Z_O44_ph2	0.12622
Biso_O3_ph1	1.373	Biso_O19_ph2	1.871	Biso_O44_ph2	1.713
Occ_O3_ph1	1	Occ_O19_ph2	1	Occ_O44_ph2	1
X_O4_ph1	0.25	X_O20_ph2	0.47258	X_O45_ph2	0.4973
Y_O4_ph1	0.75	Y_O20_ph2	0.15725	Y_O45_ph2	0.155
Z_O4_ph1	0.0008	Z_O20_ph2	0.07648	Z_O45_ph2	0.1807
Biso_O4_ph1	1.002	Biso_O20_ph2	1.555	Biso_O45_ph2	2.423
Occ_O4_ph1	1	Occ_O20_ph2	1	Occ_O45_ph2	1
Bover_ph2_pat1	0	X_O21_ph2	0.49048	X_O46_ph2	0.5101
Strain1_ph2_pat1	0	Y_O21_ph2	0.39627	Y_O46_ph2	0.492
Strain2_ph2_pat1	0	Z_O21_ph2	0.12804	Z_O46_ph2	0.1707
Strain3_ph2_pat1	0	Biso_O21_ph2	1.618	Biso_O46_ph2	2.55
G-Size_ph2_pat1	0	Occ_O21_ph2	1	Occ_O46_ph2	1
L-Size_ph2_pat1	0	X_O22_ph2	0.4726	X_O47_ph2	0.3362
Y-cos_ph2_pat1	0	Y_O22_ph2	0.48128	Y_O47_ph2	0.3271
EtaRght0_ph2_pat1	0	Z_O22_ph2	0.07129	Z_O47_ph2	0.173
X-tan_ph2_pat1	0.0216357	Biso_O22_ph2	1.823	Biso_O47_ph2	2.866
U-Cagl_ph2_pat1	0	Occ_O22_ph2	1	Occ_O47_ph2	1
V-Cagl_ph2_pat1	0	X_O23_ph2	0.41032	X_O48_ph2	0.3357
W-Cagl_ph2_pat1	0.00850576	Y_O23_ph2	0.45904	Y_O48_ph2	0.1759
EtaPV_ph2_pat1	0.0645069	Z_O23_ph2	0.15181	Z_O48_ph2	0.0004
Cell_A_ph2_pat1	26.3227	Biso_O23_ph2	1.594	Biso_O48_ph2	2.645
Cell_B_ph2_pat1	26.3227	Occ_O23_ph2	1	Occ_O48_ph2	1
Cell_C_ph2_pat1	26.3227	X_O24_ph2	0.3524	X_O49_ph2	0.16284
Cell_D_ph2_pat1	90	Y_O24_ph2	0.3083	Y_O49_ph2	0.16284
Cell_E_ph2_pat1	90	Z_O24_ph2	0.06917	Z_O49_ph2	0.16284
Cell_F_ph2_pat1	90	Biso_O24_ph2	2.044	Biso_O49_ph2	2.842
Or1_ph2_pat1	0	Occ_O24_ph2	1	Occ_O49_ph2	1
Or2_ph2_pat1	0	X_O25_ph2	0.3565	X_O50_ph2	0.5
Asym1_ph2_pat1	0.0707913	Y_O25_ph2	0.22994	Y_O50_ph2	0.5
Asym2_ph2_pat1	0	Z_O25_ph2	0.1359	Z_O50_ph2	0.5
Asym3_ph2_pat1	0	Biso_O25_ph2	2.218	Biso_O50_ph2	2.85
Asym4_ph2_pat1	0	Occ_O25_ph2	1	Occ_O50_ph2	1
X_Zr1_ph2	0.497434	X_O26_ph2	0.43193	Bover_ph3_pat1	0
Y_Zr1_ph2	-0.001114	Y_O26_ph2	0.3013	Strain1_ph3_pat1	0
Z_Zr1_ph2	0.165602	Z_O26_ph2	0.13571	Strain2_ph3_pat1	0
Biso_Zr1_ph2	0.497	Biso_O26_ph2	1.91	Strain3_ph3_pat1	0
Occ_Zr1_ph2	1	Occ_O26_ph2	1	G-Size_ph3_pat1	0
X_Zr2_ph2	0.500084	X_O27_ph2	0.23557	L-Size_ph3_pat1	0
Y_Zr2_ph2	0.32661	Y_O27_ph2	0.3606	Y-cos_ph3_pat1	0
Z_Zr2_ph2	0.164329	Z_O27_ph2	0.18436	EtaRght0_ph3_pat1	0
Biso_Zr2_ph2	0.481	Biso_O27_ph2	1.879	X-tan_ph3_pat1	0.0165867
Occ_Zr2_ph2	1	Occ_O27_ph2	1	U-Cagl_ph3_pat1	0
X_Zr3_ph2	0.496217	X_O28_ph2	0.3133	V-Cagl_ph3_pat1	0
Y_Zr3_ph2	0.170143	Y_O28_ph2	0.42848	W-Cagl_ph3_pat1	0.322872

Z_Zr3_ph2	0.34384	Z_O28_ph2	0.1951	EtaPV_ph3_pat1	0.420966
Biso_Zr3_ph2	0.426	Biso_O28_ph2	2.029	Cell_A_ph3_pat1	5.14452
Occ_Zr3_ph2	1	Occ_O28_ph2	1	Cell_B_ph3_pat1	5.19371
X_Zr4_ph2	0.331355	X_O29_ph2	0.29834	Cell_C_ph3_pat1	5.31993
Y_Zr4_ph2	0.162024	Y_O29_ph2	0.35604	Cell_D_ph3_pat1	90
Z_Zr4_ph2	0.166102	Z_O29_ph2	0.26787	Cell_E_ph3_pat1	98.8951
Biso_Zr4_ph2	0.505	Biso_O29_ph2	1.831	Cell_F_ph3_pat1	90
Occ_Zr4_ph2	1	Occ_O29_ph2	1	Or1_ph3_pat1	0
X_Zr5_ph2	0.334645	X_O30_ph2	0.3018	Or2_ph3_pat1	0
Y_Zr5_ph2	0.334645	Y_O30_ph2	0.14271	Asym1_ph3_pat1	0.002357
Z_Zr5_ph2	0.334645	Z_O30_ph2	0.09573	Asym2_ph3_pat1	0
Biso_Zr5_ph2	0.536	Biso_O30_ph2	1.792	Asym3_ph3_pat1	0
Occ_Zr5_ph2	1	Occ_O30_ph2	1	Asym4_ph3_pat1	0
X_Zr6_ph2	0	X_O31_ph2	0.24174	X_Zr1_ph3	0.2758
Y_Zr6_ph2	0	Y_O31_ph2	0.12759	Y_Zr1_ph3	0.0411
Z_Zr6_ph2	0	Z_O31_ph2	0.01154	Z_Zr1_ph3	0.2082
Biso_Zr6_ph2	0.505	Biso_O31_ph2	1.65	Biso_Zr1_ph3	0.303
Occ_Zr6_ph2	1	Occ_O31_ph2	1	Occ_Zr1_ph3	1
X_V7_ph2	0.46207	X_O32_ph2	0.32893	X_O2_ph3	0.0703
Y_V7_ph2	0.12653	Y_O32_ph2	0.07216	Y_O2_ph3	0.3359
Z_V7_ph2	0.13145	Z_O32_ph2	0.02455	Z_O2_ph3	0.3406
Biso_V7_ph2	0.781	Biso_O32_ph2	1.689	Biso_O2_ph3	0.316
Occ_V7_ph2	1	Occ_O32_ph2	1	Occ_O2_ph3	1
X_V8_ph2	0.4703	X_O33_ph2	0.35597	X_O3_ph3	0.4423
Y_V8_ph2	0.45683	Y_O33_ph2	0.27237	Y_O3_ph3	0.7549
Z_V8_ph2	0.12993	Z_O33_ph2	-0.03702	Z_O3_ph3	0.4789
Biso_V8_ph2	0.742	Biso_O33_ph2	1.587	Biso_O3_ph3	0.228
Occ_V8_ph2	1	Occ_O33_ph2	1	Occ_O3_ph3	1
X_V9_ph2	0.36952	X_O34_ph2	0.43498		

Phase Analysis Report.
Sample: solid-state 180’ 20 h × 3

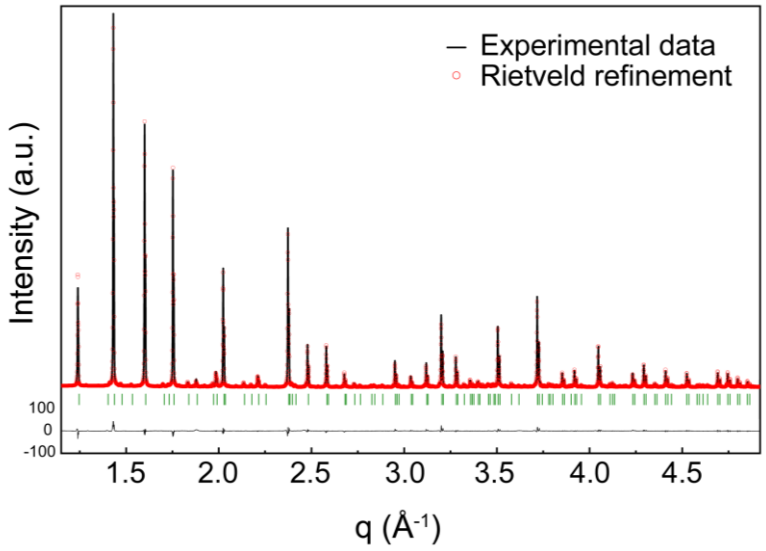

Figure S3. Rietveld refinement plot, showing the observed (black), calculated (red) and difference patterns of ZrV_2O_7 solid-state 180’ 20 h × 3 sample. Vertical lines indicate the positions of the Bragg reflections.

Sample and refinement data

Data range	15.552° - 75.029° 2Θ
Original data range	5.000° - 99.985°
Step size	0.010
Rietveld refinement converged	Yes
α2 subtracted	No
Background subtracted	No
Data smoothed	No
Specimen displacement correction (Bragg-Brentano geometry)	T = (-s/R) = 0.00023286
Radiation	X-rays
Method	Rietveld refinement
Automatic refinement	No
Final weighted average Bragg R factor	5.6
Final reduced chi^2	14.7

Matched phases

Amount (%)	Name	Formula sum	COD ID
95.5		O7 V2 Zr	2002983
4.5	Baddeleyite	O2 Zr	9007485
3.6	Unidentified peak area		

Parameter List for Refinement

Parameter	Final value	Parameter	Final value	Parameter	Final value
SyCos_pat1	0.0266838	Biso_V14_ph1	0.726	Biso_O36_ph1	1.744
Bck_0_pat1	0.999296	Occ_V14_ph1	1	Occ_O36_ph1	1
Scale_ph1_pat1	1.74401E-06	X_V15_ph1	0.20147	X_O37_ph1	0.51715
Cell_A_ph1_pat1	26.3254	Y_V15_ph1	0.20147	Y_O37_ph1	0.59745
Scale_ph2_pat1	0.000709882	Z_V15_ph1	0.20147	Z_O37_ph1	0.18395
Cell_A_ph2_pat1	5.14671	Biso_V15_ph1	0.813	Biso_O37_ph1	1.871
Cell_B_ph2_pat1	5.20834	Occ_V15_ph1	1	Occ_O37_ph1	1
Cell_C_ph2_pat1	5.31561	X_V16_ph1	0.53834	X_O38_ph1	0.60074
Cell_E_ph2_pat1	99.201	Y_V16_ph1	0.53834	Y_O38_ph1	0.53739
Zero_pat1	0	Z_V16_ph1	0.53834	Z_O38_ph1	0.20051
SySin_pat1	0	Biso_V16_ph1	0.686	Biso_O38_ph1	1.808
Lambda_pat1	1.54187	Occ_V16_ph1	1	Occ_O38_ph1	1
P0_mabs_pat1	0	X_V17_ph1	0.12459	X_O39_ph1	0.51072
Cp_mabs_pat1	0	Y_V17_ph1	0.12459	Y_O39_ph1	0.25854
Tau_mabs_pat1	0.1	Z_V17_ph1	0.12459	Z_O39_ph1	0.20207
Bck_1_pat1	0	Biso_V17_ph1	0.734	Biso_O39_ph1	1.823
Bck_2_pat1	0	Occ_V17_ph1	1	Occ_O39_ph1	1
Bck_3_pat1	0	X_O18_ph1	0.48004	X_O40_ph1	0.59407
Bover_ph1_pat1	0	Y_O18_ph1	0.06539	Y_O40_ph1	0.19718
Strain1_ph1_pat1	0	Z_O18_ph1	0.1262	Z_O40_ph1	0.19242
Strain2_ph1_pat1	0	Biso_O18_ph1	1.523	Biso_O40_ph1	1.808
Strain3_ph1_pat1	0	Occ_O18_ph1	1	Occ_O40_ph1	1
G-Size_ph1_pat1	0	X_O19_ph1	0.40009	X_O41_ph1	0.5323
L-Size_ph1_pat1	0	Y_O19_ph1	0.12892	Y_O41_ph1	0.18804
Y-cos_ph1_pat1	0	Z_O19_ph1	0.1466	Z_O41_ph1	0.2758
EtaRght0_ph1_pat1	0	Biso_O19_ph1	1.871	Biso_O41_ph1	1.847
X-tan_ph1_pat1	0.00773469	Occ_O19_ph1	1	Occ_O41_ph1	1
U-Cagl_ph1_pat1	0	X_O20_ph1	0.47258	X_O42_ph1	0.26222
V-Cagl_ph1_pat1	0	Y_O20_ph1	0.15725	Y_O42_ph1	0.1951
W-Cagl_ph1_pat1	0.0021958	Z_O20_ph1	0.07648	Z_O42_ph1	0.18376

EtaPV_ph1_pat1	0.304948	Biso_O20_ph1	1.555	Biso_O42_ph1	1.958
Cell_B_ph1_pat1	26.3254	Occ_O20_ph1	1	Occ_O42_ph1	1
Cell_C_ph1_pat1	26.3254	X_O21_ph1	0.49048	X_O43_ph1	0.59815
Cell_D_ph1_pat1	90	Y_O21_ph1	0.39627	Y_O43_ph1	-0.01624
Cell_E_ph1_pat1	90	Z_O21_ph1	0.12804	Z_O43_ph1	0.03707
Cell_F_ph1_pat1	90	Biso_O21_ph1	1.618	Biso_O43_ph1	1.531
Or1_ph1_pat1	0	Occ_O21_ph1	1	Occ_O43_ph1	1
Or2_ph1_pat1	0	X_O22_ph1	0.4726	X_O44_ph1	0.06452
Asym1_ph1_pat1	0	Y_O22_ph1	0.48128	Y_O44_ph1	0.14578
Asym2_ph1_pat1	0.0281335	Z_O22_ph1	0.07129	Z_O44_ph1	0.12622
Asym3_ph1_pat1	0	Biso_O22_ph1	1.823	Biso_O44_ph1	1.713
Asym4_ph1_pat1	0	Occ_O22_ph1	1	Occ_O44_ph1	1
X_Zr1_ph1	0.497434	X_O23_ph1	0.41032	X_O45_ph1	0.4973
Y_Zr1_ph1	-0.001114	Y_O23_ph1	0.45904	Y_O45_ph1	0.155
Z_Zr1_ph1	0.165602	Z_O23_ph1	0.15181	Z_O45_ph1	0.1807
Biso_Zr1_ph1	1.39768	Biso_O23_ph1	1.594	Biso_O45_ph1	2.423
Occ_Zr1_ph1	1	Occ_O23_ph1	1	Occ_O45_ph1	1
X_Zr2_ph1	0.50008	X_O24_ph1	0.3524	X_O46_ph1	0.5101
Y_Zr2_ph1	0.32661	Y_O24_ph1	0.3083	Y_O46_ph1	0.492
Z_Zr2_ph1	0.164329	Z_O24_ph1	0.06917	Z_O46_ph1	0.1707
Biso_Zr2_ph1	1.68529	Biso_O24_ph1	2.044	Biso_O46_ph1	2.55
Occ_Zr2_ph1	1	Occ_O24_ph1	1	Occ_O46_ph1	1
X_Zr3_ph1	0.496217	X_O25_ph1	0.3565	X_O47_ph1	0.3362
Y_Zr3_ph1	0.170143	Y_O25_ph1	0.22994	Y_O47_ph1	0.3271
Z_Zr3_ph1	0.34384	Z_O25_ph1	0.1359	Z_O47_ph1	0.173
Biso_Zr3_ph1	1.0166	Biso_O25_ph1	2.218	Biso_O47_ph1	2.866
Occ_Zr3_ph1	1	Occ_O25_ph1	1	Occ_O47_ph1	1
X_Zr4_ph1	0.331355	X_O26_ph1	0.43193	X_O48_ph1	0.3357
Y_Zr4_ph1	0.162024	Y_O26_ph1	0.3013	Y_O48_ph1	0.1759
Z_Zr4_ph1	0.1661	Z_O26_ph1	0.13571	Z_O48_ph1	0.0004
Biso_Zr4_ph1	0.38058	Biso_O26_ph1	1.91	Biso_O48_ph1	2.645
Occ_Zr4_ph1	1	Occ_O26_ph1	1	Occ_O48_ph1	1

X_Zr5_ph1	0.334645	X_O27_ph1	0.23557	X_O49_ph1	0.16284
Y_Zr5_ph1	0.334645	Y_O27_ph1	0.3606	Y_O49_ph1	0.16284
Z_Zr5_ph1	0.334645	Z_O27_ph1	0.18436	Z_O49_ph1	0.16284
Biso_Zr5_ph1	0.50051	Biso_O27_ph1	1.879	Biso_O49_ph1	2.842
Occ_Zr5_ph1	1	Occ_O27_ph1	1	Occ_O49_ph1	1
X_Zr6_ph1	0	X_O28_ph1	0.3133	X_O50_ph1	0.5
Y_Zr6_ph1	0	Y_O28_ph1	0.42848	Y_O50_ph1	0.5
Z_Zr6_ph1	0	Z_O28_ph1	0.1951	Z_O50_ph1	0.5
Biso_Zr6_ph1	0.081808	Biso_O28_ph1	2.029	Biso_O50_ph1	2.85
Occ_Zr6_ph1	1	Occ_O28_ph1	1	Occ_O50_ph1	1
X_V7_ph1	0.46207	X_O29_ph1	0.29834	Bover_ph2_pat1	0
Y_V7_ph1	0.12653	Y_O29_ph1	0.35604	Strain1_ph2_pat1	0
Z_V7_ph1	0.13145	Z_O29_ph1	0.26787	Strain2_ph2_pat1	0
Biso_V7_ph1	0.781	Biso_O29_ph1	1.831	Strain3_ph2_pat1	0
Occ_V7_ph1	1	Occ_O29_ph1	1	G-Size_ph2_pat1	0
X_V8_ph1	0.4703	X_O30_ph1	0.3018	L-Size_ph2_pat1	0
Y_V8_ph1	0.45683	Y_O30_ph1	0.14271	Y-cos_ph2_pat1	0
Z_V8_ph1	0.12993	Z_O30_ph1	0.09573	EtaRght0_ph2_pat1	0
Biso_V8_ph1	0.742	Biso_O30_ph1	1.792	X-tan_ph2_pat1	0.014973
Occ_V8_ph1	1	Occ_O30_ph1	1	U-Cagl_ph2_pat1	0
X_V9_ph1	0.36952	X_O31_ph1	0.24174	V-Cagl_ph2_pat1	0
Y_V9_ph1	0.29152	Y_O31_ph1	0.12759	W-Cagl_ph2_pat1	0.0052784 6
Z_V9_ph1	0.12774	Z_O31_ph1	0.01154	EtaPV_ph2_pat1	0.235389
Biso_V9_ph1	0.742	Biso_O31_ph1	1.65	Cell_D_ph2_pat1	90
Occ_V9_ph1	1	Occ_O31_ph1	1	Cell_F_ph2_pat1	90
X_V10_ph1	0.29521	X_O32_ph1	0.32893	Or1_ph2_pat1	0
Y_V10_ph1	0.36857	Y_O32_ph1	0.07216	Or2_ph2_pat1	0
Z_V10_ph1	0.20539	Z_O32_ph1	0.02455	Asym1_ph2_pat1	0
Biso_V10_ph1	0.757	Biso_O32_ph1	1.689	Asym2_ph2_pat1	0
Occ_V10_ph1	1	Occ_O32_ph1	1	Asym3_ph2_pat1	0

X_V11_ph1	0.30164	X_O33_ph1	0.35597	Asym4_ph2_pat1	0
Y_V11_ph1	0.12878	Y_O33_ph1	0.27237	X_Zr1_ph2	0.2758
Z_V11_ph1	0.03361	Z_O33_ph1	-0.03702	Y_Zr1_ph2	0.0411
Biso_V11_ph1	0.679	Biso_O33_ph1	1.587	Z_Zr1_ph2	0.2082
Occ_V11_ph1	1	Occ_O33_ph1	1	Biso_Zr1_ph2	0.303
X_V12_ph1	0.37478	X_O34_ph1	0.43498	Occ_Zr1_ph2	1
Y_V12_ph1	0.21139	Y_O34_ph1	0.20653	X_O2_ph2	0.0703
Z_V12_ph1	-0.0395	Z_O34_ph1	-0.01851	Y_O2_ph2	0.3359
Biso_V12_ph1	0.765	Biso_O34_ph1	1.721	Z_O2_ph2	0.3406
Occ_V12_ph1	1	Occ_O34_ph1	1	Biso_O2_ph2	0.316
X_V13_ph1	0.53727	X_O35_ph1	0.37015	Occ_O2_ph2	1
Y_V13_ph1	0.54143	Y_O35_ph1	0.18931	X_O3_ph2	0.4423
Z_V13_ph1	0.20594	Z_O35_ph1	-0.09934	Y_O3_ph2	0.7549
Biso_V13_ph1	0.757	Biso_O35_ph1	1.808	Z_O3_ph2	0.4789
Occ_V13_ph1	1	Occ_O35_ph1	1	Biso_O3_ph2	0.228
X_V14_ph1	0.53403	X_O36_ph1	0.5206	Occ_O3_ph2	1
Y_V14_ph1	0.20035	Y_O36_ph1	0.53508		
Z_V14_ph1	0.21313	Z_O36_ph1	0.26734		

Phase Analysis Report.
Sample: solid-state 40’ 5 h N_2-quenched

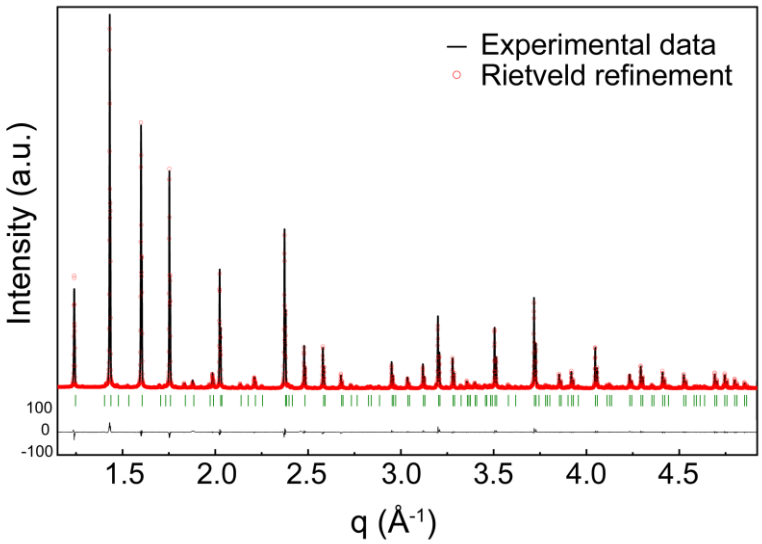

Figure S4. Rietveld refinement plot, showing the observed (black), calculated (red) and difference patterns of ZrV_2O_7 solid-state 40’ 5 h N_2-quenched sample. Vertical lines indicate the positions of the Bragg reflections.

Sample and refinement data

Data range	14.627° - 74.319° 2Θ
Original data range	5.000° - 99.985°
Step size	0.010
Rietveld refinement converged	Yes
α2 subtracted	No
Background subtracted	No
Data smoothed	No
Specimen displacement correction (Bragg-Brentano geometry)	T = (-s/R) = 0.0010909
Radiation	X-rays
Method	Rietveld refinement
Automatic refinement	No
Final weighted average Bragg R factor	6.1
Final reduced chi^2	13.3

Matched phases

Amount (%)	Name	Formula sum	COD ID
76.4		O7 V2 Zr	2002983
13.4	Shcherbinaite	O5 V2	9012221
10.2	Baddeleyite	O2 Zr	9007485
4.4	Unidentified peak area		

Parameter List for Refinement

Parameter	Final value	Parameter	Final value	Parameter	Final value
SyCos_pat1	0.125007	Occ_V16_ph1	1	Occ_O41_ph1	1
Bck_2_pat1	0.0145723	X_V17_ph1	0.12459	X_O42_ph1	0.26222
Scale_ph1_pat1	9.87702E-07	Y_V17_ph1	0.12459	Y_O42_ph1	0.1951
Cell_A_ph1_pat1	26.3199	Z_V17_ph1	0.12459	Z_O42_ph1	0.18376
Asym2_ph1_pat1	0.0184983	Biso_V17_ph1	0.734	Biso_O42_ph1	1.958
Scale_ph2_pat1	0.00160114	Occ_V17_ph1	1	Occ_O42_ph1	1
Cell_A_ph2_pat1	11.5078	X_O18_ph1	0.48004	X_O43_ph1	0.59815
Cell_B_ph2_pat1	3.55543	Y_O18_ph1	0.06539	Y_O43_ph1	-0.01624
Cell_C_ph2_pat1	4.37343	Z_O18_ph1	0.1262	Z_O43_ph1	0.03707
Scale_ph3_pat1	0.00114248	Biso_O18_ph1	1.523	Biso_O43_ph1	1.531
Cell_A_ph3_pat1	5.14906	Occ_O18_ph1	1	Occ_O43_ph1	1
Cell_B_ph3_pat1	5.20791	X_O19_ph1	0.40009	X_O44_ph1	0.06452
Cell_C_ph3_pat1	5.31993	Y_O19_ph1	0.12892	Y_O44_ph1	0.14578
Cell_E_ph3_pat1	99.2095	Z_O19_ph1	0.1466	Z_O44_ph1	0.12622
Zero_pat1	0	Biso_O19_ph1	1.871	Biso_O44_ph1	1.713
SySin_pat1	0	Occ_O19_ph1	1	Occ_O44_ph1	1
Lambda_pat1	1.54187	X_O20_ph1	0.47258	X_O45_ph1	0.4973
P0_mabs_pat1	0	Y_O20_ph1	0.15725	Y_O45_ph1	0.155
Cp_mabs_pat1	0	Z_O20_ph1	0.07648	Z_O45_ph1	0.1807
Tau_mabs_pat1	0.1	Biso_O20_ph1	1.555	Biso_O45_ph1	2.423
Bck_0_pat1	1.00414	Occ_O20_ph1	1	Occ_O45_ph1	1
Bck_1_pat1	-16.0878	X_O21_ph1	0.49048	X_O46_ph1	0.5101
Bck_3_pat1	0	Y_O21_ph1	0.39627	Y_O46_ph1	0.492
Bover_ph1_pat1	0	Z_O21_ph1	0.12804	Z_O46_ph1	0.1707
Strain1_ph1_pat1	0	Biso_O21_ph1	1.618	Biso_O46_ph1	2.55
Strain2_ph1_pat1	0	Occ_O21_ph1	1	Occ_O46_ph1	1
Strain3_ph1_pat1	0	X_O22_ph1	0.4726	X_O47_ph1	0.3362
G-Size_ph1_pat1	0	Y_O22_ph1	0.48128	Y_O47_ph1	0.3271
L-Size_ph1_pat1	0	Z_O22_ph1	0.07129	Z_O47_ph1	0.173
Y-cos_ph1_pat1	0	Biso_O22_ph1	1.823	Biso_O47_ph1	2.866
EtaRght0_ph1_pat1	0	Occ_O22_ph1	1	Occ_O47_ph1	1
X-tan_ph1_pat1	0.0183281	X_O23_ph1	0.41032	X_O48_ph1	0.3357
U-Cagl_ph1_pat1	0	Y_O23_ph1	0.45904	Y_O48_ph1	0.1759
V-Cagl_ph1_pat1	0	Z_O23_ph1	0.15181	Z_O48_ph1	0.0004
W-Cagl_ph1_pat1	0.00499782	Biso_O23_ph1	1.594	Biso_O48_ph1	2.645
EtaPV_ph1_pat1	0.142145	Occ_O23_ph1	1	Occ_O48_ph1	1
Cell_B_ph1_pat1	26.3199	X_O24_ph1	0.3524	X_O49_ph1	0.16284
Cell_C_ph1_pat1	26.3199	Y_O24_ph1	0.3083	Y_O49_ph1	0.16284
Cell_D_ph1_pat1	90	Z_O24_ph1	0.06917	Z_O49_ph1	0.16284
Cell_E_ph1_pat1	90	Biso_O24_ph1	2.044	Biso_O49_ph1	2.842
Cell_F_ph1_pat1	90	Occ_O24_ph1	1	Occ_O49_ph1	1
Or1_ph1_pat1	0	X_O25_ph1	0.3565	X_O50_ph1	0.5
Or2_ph1_pat1	0	Y_O25_ph1	0.22994	Y_O50_ph1	0.5
Asym1_ph1_pat1	0	Z_O25_ph1	0.1359	Z_O50_ph1	0.5
Asym3_ph1_pat1	0	Biso_O25_ph1	2.218	Biso_O50_ph1	2.85
Asym4_ph1_pat1	0	Occ_O25_ph1	1	Occ_O50_ph1	1

X_Zr1_ph1	0.497434	X_O26_ph1	0.43193	Bover_ph2_pat1	0
Y_Zr1_ph1	-0.001114	Y_O26_ph1	0.3013	Strain1_ph2_pat1	0
Z_Zr1_ph1	0.165602	Z_O26_ph1	0.13571	Strain2_ph2_pat1	0
Biso_Zr1_ph1	0.497	Biso_O26_ph1	1.91	Strain3_ph2_pat1	0
Occ_Zr1_ph1	1	Occ_O26_ph1	1	G-Size_ph2_pat1	0
X_Zr2_ph1	0.500084	X_O27_ph1	0.23557	L-Size_ph2_pat1	0
Y_Zr2_ph1	0.32661	Y_O27_ph1	0.3606	Y-cos_ph2_pat1	0
Z_Zr2_ph1	0.164329	Z_O27_ph1	0.18436	EtaRght0_ph2_pat1	0
Biso_Zr2_ph1	0.481	Biso_O27_ph1	1.879	X-tan_ph2_pat1	0.0296979
Occ_Zr2_ph1	1	Occ_O27_ph1	1	U-Cagl_ph2_pat1	0
X_Zr3_ph1	0.496217	X_O28_ph1	0.3133	V-Cagl_ph2_pat1	0
Y_Zr3_ph1	0.170143	Y_O28_ph1	0.42848	W-Cagl_ph2_pat1	0.0179067
Z_Zr3_ph1	0.34384	Z_O28_ph1	0.1951	EtaPV_ph2_pat1	0.142823
Biso_Zr3_ph1	0.426	Biso_O28_ph1	2.029	Cell_D_ph2_pat1	90
Occ_Zr3_ph1	1	Occ_O28_ph1	1	Cell_E_ph2_pat1	90
X_Zr4_ph1	0.331355	X_O29_ph1	0.29834	Cell_F_ph2_pat1	90
Y_Zr4_ph1	0.162024	Y_O29_ph1	0.35604	Or1_ph2_pat1	0
Z_Zr4_ph1	0.166102	Z_O29_ph1	0.26787	Or2_ph2_pat1	0
Biso_Zr4_ph1	0.505	Biso_O29_ph1	1.831	Asym1_ph2_pat1	0.054126
Occ_Zr4_ph1	1	Occ_O29_ph1	1	Asym2_ph2_pat1	0
X_Zr5_ph1	0.334645	X_O30_ph1	0.3018	Asym3_ph2_pat1	0
Y_Zr5_ph1	0.334645	Y_O30_ph1	0.14271	Asym4_ph2_pat1	0
Z_Zr5_ph1	0.334645	Z_O30_ph1	0.09573	X_V1_ph2	0.60123
Biso_Zr5_ph1	0.536	Biso_O30_ph1	1.792	Y_V1_ph2	0.25
Occ_Zr5_ph1	1	Occ_O30_ph1	1	Z_V1_ph2	0.1086
X_Zr6_ph1	0	X_O31_ph1	0.24174	Biso_V1_ph2	0.592
Y_Zr6_ph1	0	Y_O31_ph1	0.12759	Occ_V1_ph2	1
Z_Zr6_ph1	0	Z_O31_ph1	0.01154	X_O2_ph2	0.4309
Biso_Zr6_ph1	0.505	Biso_O31_ph1	1.65	Y_O2_ph2	0.25
Occ_Zr6_ph1	1	Occ_O31_ph1	1	Z_O2_ph2	-0.0028
X_V7_ph1	0.46207	X_O32_ph1	0.32893	Biso_O2_ph2	0.781
Y_V7_ph1	0.12653	Y_O32_ph1	0.07216	Occ_O2_ph2	1
Z_V7_ph1	0.13145	Z_O32_ph1	0.02455	X_O3_ph2	0.6045
Biso_V7_ph1	0.781	Biso_O32_ph1	1.689	Y_O3_ph2	0.25
Occ_V7_ph1	1	Occ_O32_ph1	1	Z_O3_ph2	0.4697
X_V8_ph1	0.4703	X_O33_ph1	0.35597	Biso_O3_ph2	1.373
Y_V8_ph1	0.45683	Y_O33_ph1	0.27237	Occ_O3_ph2	1
Z_V8_ph1	0.12993	Z_O33_ph1	-0.03702	X_O4_ph2	0.25
Biso_V8_ph1	0.742	Biso_O33_ph1	1.587	Y_O4_ph2	0.75
Occ_V8_ph1	1	Occ_O33_ph1	1	Z_O4_ph2	0.0008
X_V9_ph1	0.36952	X_O34_ph1	0.43498	Biso_O4_ph2	1.002
Y_V9_ph1	0.29152	Y_O34_ph1	0.20653	Occ_O4_ph2	1
Z_V9_ph1	0.12774	Z_O34_ph1	-0.01851	Bover_ph3_pat1	0
Biso_V9_ph1	0.742	Biso_O34_ph1	1.721	Strain1_ph3_pat1	0
Occ_V9_ph1	1	Occ_O34_ph1	1	Strain2_ph3_pat1	0
X_V10_ph1	0.29521	X_O35_ph1	0.37015	Strain3_ph3_pat1	0
Y_V10_ph1	0.36857	Y_O35_ph1	0.18931	G-Size_ph3_pat1	0

Z_V10_ph1	0.20539	Z_O35_ph1	-0.09934	L-Size_ph3_pat1	0
Biso_V10_ph1	0.757	Biso_O35_ph1	1.808	Y-cos_ph3_pat1	0
Occ_V10_ph1	1	Occ_O35_ph1	1	EtaRght0_ph3_pat1	0
X_V11_ph1	0.30164	X_O36_ph1	0.5206	X-tan_ph3_pat1	0.0118651
Y_V11_ph1	0.12878	Y_O36_ph1	0.53508	U-Cagl_ph3_pat1	0
Z_V11_ph1	0.03361	Z_O36_ph1	0.26734	V-Cagl_ph3_pat1	0
Biso_V11_ph1	0.679	Biso_O36_ph1	1.744	W-Cagl_ph3_pat1	0.00898257
Occ_V11_ph1	1	Occ_O36_ph1	1	EtaPV_ph3_pat1	0.28069
X_V12_ph1	0.37478	X_O37_ph1	0.51715	Cell_D_ph3_pat1	90
Y_V12_ph1	0.21139	Y_O37_ph1	0.59745	Cell_F_ph3_pat1	90
Z_V12_ph1	-0.0395	Z_O37_ph1	0.18395	Or1_ph3_pat1	0
Biso_V12_ph1	0.765	Biso_O37_ph1	1.871	Or2_ph3_pat1	0
Occ_V12_ph1	1	Occ_O37_ph1	1	Asym1_ph3_pat1	0
X_V13_ph1	0.53727	X_O38_ph1	0.60074	Asym2_ph3_pat1	0
Y_V13_ph1	0.54143	Y_O38_ph1	0.53739	Asym3_ph3_pat1	0
Z_V13_ph1	0.20594	Z_O38_ph1	0.20051	Asym4_ph3_pat1	0
Biso_V13_ph1	0.757	Biso_O38_ph1	1.808	X_Zr1_ph3	0.2758
Occ_V13_ph1	1	Occ_O38_ph1	1	Y_Zr1_ph3	0.0411
X_V14_ph1	0.53403	X_O39_ph1	0.51072	Z_Zr1_ph3	0.2082
Y_V14_ph1	0.20035	Y_O39_ph1	0.25854	Biso_Zr1_ph3	0.303
Z_V14_ph1	0.21313	Z_O39_ph1	0.20207	Occ_Zr1_ph3	1
Biso_V14_ph1	0.726	Biso_O39_ph1	1.823	X_O2_ph3	0.0703
Occ_V14_ph1	1	Occ_O39_ph1	1	Y_O2_ph3	0.3359
X_V15_ph1	0.20147	X_O40_ph1	0.59407	Z_O2_ph3	0.3406
Y_V15_ph1	0.20147	Y_O40_ph1	0.19718	Biso_O2_ph3	0.316
Z_V15_ph1	0.20147	Z_O40_ph1	0.19242	Occ_O2_ph3	1
Biso_V15_ph1	0.813	Biso_O40_ph1	1.808	X_O3_ph3	0.4423
Occ_V15_ph1	1	Occ_O40_ph1	1	Y_O3_ph3	0.7549
X_V16_ph1	0.53834	X_O41_ph1	0.5323	Z_O3_ph3	0.4789
Y_V16_ph1	0.53834	Y_O41_ph1	0.18804	Biso_O3_ph3	0.228
Z_V16_ph1	0.53834	Z_O41_ph1	0.2758	Occ_O3_ph3	1
Biso_V16_ph1	0.686	Biso_O41_ph1	1.847		

Phase Analysis Report.
Sample: solvothermal

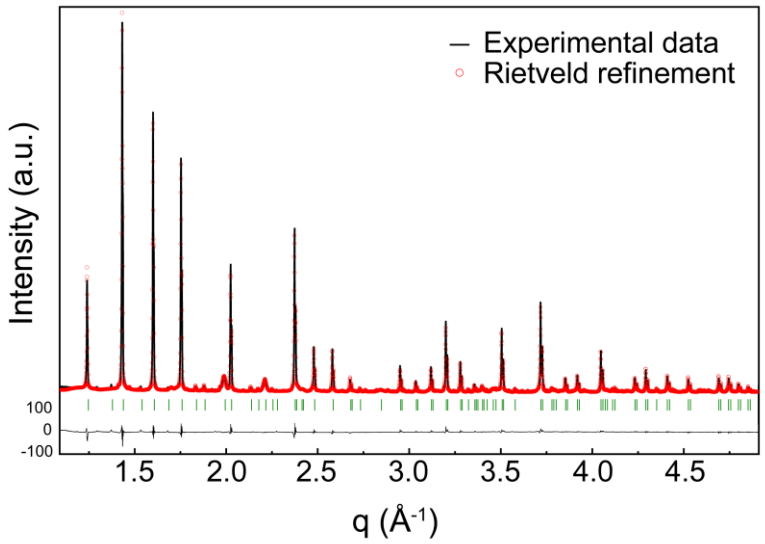

Figure S5. Rietveld refinement plot, showing the observed (black), calculated (red) and difference patterns of ZrV_2O_7 solvothermal reaction sample. Vertical lines indicate the positions of the Bragg reflections.

Sample and refinement data

Data range	15.415° - 74.141° 2Θ
Original data range	5.000° - 99.985°
Step size	0.010
Rietveld refinement converged	Yes
α2 subtracted	No
Background subtracted	No
Data smoothed	No
Specimen displacement correction (Bragg-Brentano geometry)	T = (-s/R) = 0.00044662
Radiation	X-rays
Method	Rietveld refinement
Automatic refinement	No
Final weighted average Bragg R factor	8.0
Final reduced chi^2	17.2

Matched phases

Amount (%)	Name	Formula sum	COD ID
90.4		O7 V2 Zr	2002983
9.6	Baddeleyite	O2 Zr	9007485
4.6	Unidentified peak area		

Parameter List for Refinement

Parameter	Final value	Parameter	Final value	Parameter	Final value
SyCos_pat1	0.0511788	Z_V14_ph1	0.21313	Y_O36_ph1	0.53508
Bck_1_pat1	-1.51723	Biso_V14_ph1	0.726	Z_O36_ph1	0.26734
Scale_ph1_pat1	1.0232E-06	Occ_V14_ph1	1	Biso_O36_ph1	1.744
Cell_A_ph1_pat1	26.3263	X_V15_ph1	0.20147	Occ_O36_ph1	1
Scale_ph2_pat1	0.000945713	Y_V15_ph1	0.20147	X_O37_ph1	0.51715
Cell_A_ph2_pat1	5.14198	Z_V15_ph1	0.20147	Y_O37_ph1	0.59745
Cell_B_ph2_pat1	5.19771	Biso_V15_ph1	0.813	Z_O37_ph1	0.18395
Cell_C_ph2_pat1	5.32425	Occ_V15_ph1	1	Biso_O37_ph1	1.871
Cell_E_ph2_pat1	99.0942	X_V16_ph1	0.53834	Occ_O37_ph1	1
Zero_pat1	0	Y_V16_ph1	0.53834	X_O38_ph1	0.60074
SySin_pat1	0	Z_V16_ph1	0.53834	Y_O38_ph1	0.53739
Lambda_pat1	1.54187	Biso_V16_ph1	0.686	Z_O38_ph1	0.20051
P0_mabs_pat1	0	Occ_V16_ph1	1	Biso_O38_ph1	1.808
Cp_mabs_pat1	0	X_V17_ph1	0.12459	Occ_O38_ph1	1
Tau_mabs_pat1	0.1	Y_V17_ph1	0.12459	X_O39_ph1	0.51072
Bck_0_pat1	0.999828	Z_V17_ph1	0.12459	Y_O39_ph1	0.25854
Bck_2_pat1	0	Biso_V17_ph1	0.734	Z_O39_ph1	0.20207
Bck_3_pat1	0	Occ_V17_ph1	1	Biso_O39_ph1	1.823
Bover_ph1_pat1	0.009863	X_O18_ph1	0.48004	Occ_O39_ph1	1
Strain1_ph1_pat1	0	Y_O18_ph1	0.06539	X_O40_ph1	0.59407
Strain2_ph1_pat1	0	Z_O18_ph1	0.1262	Y_O40_ph1	0.19718
Strain3_ph1_pat1	0	Biso_O18_ph1	1.523	Z_O40_ph1	0.19242
G-Size_ph1_pat1	0	Occ_O18_ph1	1	Biso_O40_ph1	1.808
L-Size_ph1_pat1	0	X_O19_ph1	0.40009	Occ_O40_ph1	1
Y-cos_ph1_pat1	0	Y_O19_ph1	0.12892	X_O41_ph1	0.5323
EtaRght0_ph1_pat1	0	Z_O19_ph1	0.1466	Y_O41_ph1	0.18804
X-tan_ph1_pat1	0.0108357	Biso_O19_ph1	1.871	Z_O41_ph1	0.2758
U-Cagl_ph1_pat1	0	Occ_O19_ph1	1	Biso_O41_ph1	1.847
V-Cagl_ph1_pat1	0	X_O20_ph1	0.47258	Occ_O41_ph1	1
W-Cagl_ph1_pat1	0.00358055	Y_O20_ph1	0.15725	X_O42_ph1	0.26222
EtaPV_ph1_pat1	0.297546	Z_O20_ph1	0.07648	Y_O42_ph1	0.1951
Cell_B_ph1_pat1	26.3263	Biso_O20_ph1	1.555	Z_O42_ph1	0.18376
Cell_C_ph1_pat1	26.3263	Occ_O20_ph1	1	Biso_O42_ph1	1.958
Cell_D_ph1_pat1	90	X_O21_ph1	0.49048	Occ_O42_ph1	1
Cell_E_ph1_pat1	90	Y_O21_ph1	0.39627	X_O43_ph1	0.59815
Cell_F_ph1_pat1	90	Z_O21_ph1	0.12804	Y_O43_ph1	-0.01624
Or1_ph1_pat1	0	Biso_O21_ph1	1.618	Z_O43_ph1	0.03707
Or2_ph1_pat1	0	Occ_O21_ph1	1	Biso_O43_ph1	1.531
Asym1_ph1_pat1	0	X_O22_ph1	0.4726	Occ_O43_ph1	1
Asym2_ph1_pat1	0.0329566	Y_O22_ph1	0.48128	X_O44_ph1	0.06452
Asym3_ph1_pat1	0	Z_O22_ph1	0.07129	Y_O44_ph1	0.14578
Asym4_ph1_pat1	0	Biso_O22_ph1	1.823	Z_O44_ph1	0.12622
X_Zr1_ph1	0.497434	Occ_O22_ph1	1	Biso_O44_ph1	1.713
Y_Zr1_ph1	-0.001114	X_O23_ph1	0.41032	Occ_O44_ph1	1
Z_Zr1_ph1	0.165602	Y_O23_ph1	0.45904	X_O45_ph1	0.4973
Biso_Zr1_ph1	0.497	Z_O23_ph1	0.15181	Y_O45_ph1	0.155
Occ_Zr1_ph1	1	Biso_O23_ph1	1.594	Z_O45_ph1	0.1807

X_Zr2_ph1	0.500084	Occ_O23_ph1	1	Biso_O45_ph1	2.423
Y_Zr2_ph1	0.32661	X_O24_ph1	0.3524	Occ_O45_ph1	1
Z_Zr2_ph1	0.164329	Y_O24_ph1	0.3083	X_O46_ph1	0.5101
Biso_Zr2_ph1	0.481	Z_O24_ph1	0.06917	Y_O46_ph1	0.492
Occ_Zr2_ph1	1	Biso_O24_ph1	2.044	Z_O46_ph1	0.1707
X_Zr3_ph1	0.496217	Occ_O24_ph1	1	Biso_O46_ph1	2.55
Y_Zr3_ph1	0.170143	X_O25_ph1	0.3565	Occ_O46_ph1	1
Z_Zr3_ph1	0.34384	Y_O25_ph1	0.22994	X_O47_ph1	0.3362
Biso_Zr3_ph1	0.426	Z_O25_ph1	0.1359	Y_O47_ph1	0.3271
Occ_Zr3_ph1	1	Biso_O25_ph1	2.218	Z_O47_ph1	0.173
X_Zr4_ph1	0.331355	Occ_O25_ph1	1	Biso_O47_ph1	2.866
Y_Zr4_ph1	0.162024	X_O26_ph1	0.43193	Occ_O47_ph1	1
Z_Zr4_ph1	0.166102	Y_O26_ph1	0.3013	X_O48_ph1	0.3357
Biso_Zr4_ph1	0.505	Z_O26_ph1	0.13571	Y_O48_ph1	0.1759
Occ_Zr4_ph1	1	Biso_O26_ph1	1.91	Z_O48_ph1	0.0004
X_Zr5_ph1	0.334645	Occ_O26_ph1	1	Biso_O48_ph1	2.645
Y_Zr5_ph1	0.334645	X_O27_ph1	0.23557	Occ_O48_ph1	1
Z_Zr5_ph1	0.334645	Y_O27_ph1	0.3606	X_O49_ph1	0.16284
Biso_Zr5_ph1	0.536	Z_O27_ph1	0.18436	Y_O49_ph1	0.16284
Occ_Zr5_ph1	1	Biso_O27_ph1	1.879	Z_O49_ph1	0.16284
X_Zr6_ph1	0	Occ_O27_ph1	1	Biso_O49_ph1	2.842
Y_Zr6_ph1	0	X_O28_ph1	0.3133	Occ_O49_ph1	1
Z_Zr6_ph1	0	Y_O28_ph1	0.42848	X_O50_ph1	0.5
Biso_Zr6_ph1	0.505	Z_O28_ph1	0.1951	Y_O50_ph1	0.5
Occ_Zr6_ph1	1	Biso_O28_ph1	2.029	Z_O50_ph1	0.5
X_V7_ph1	0.46207	Occ_O28_ph1	1	Biso_O50_ph1	2.85
Y_V7_ph1	0.12653	X_O29_ph1	0.29834	Occ_O50_ph1	1
Z_V7_ph1	0.13145	Y_O29_ph1	0.35604	Bover_ph2_pat1	1.01542
Biso_V7_ph1	0.781	Z_O29_ph1	0.26787	Strain1_ph2_pat1	0
Occ_V7_ph1	1	Biso_O29_ph1	1.831	Strain2_ph2_pat1	0
X_V8_ph1	0.4703	Occ_O29_ph1	1	Strain3_ph2_pat1	0
Y_V8_ph1	0.45683	X_O30_ph1	0.3018	G-Size_ph2_pat1	0
Z_V8_ph1	0.12993	Y_O30_ph1	0.14271	L-Size_ph2_pat1	0
Biso_V8_ph1	0.742	Z_O30_ph1	0.09573	Y-cos_ph2_pat1	0
Occ_V8_ph1	1	Biso_O30_ph1	1.792	EtaRght0_ph2_pat1	0
X_V9_ph1	0.36952	Occ_O30_ph1	1	X-tan_ph2_pat1	0
Y_V9_ph1	0.29152	X_O31_ph1	0.24174	U-Cagl_ph2_pat1	0
Z_V9_ph1	0.12774	Y_O31_ph1	0.12759	V-Cagl_ph2_pat1	0
Biso_V9_ph1	0.742	Z_O31_ph1	0.01154	W-Cagl_ph2_pat1	0.0803331
Occ_V9_ph1	1	Biso_O31_ph1	1.65	EtaPV_ph2_pat1	0.29754
X_V10_ph1	0.29521	Occ_O31_ph1	1	Cell_D_ph2_pat1	90
Y_V10_ph1	0.36857	X_O32_ph1	0.32893	Cell_F_ph2_pat1	90
Z_V10_ph1	0.20539	Y_O32_ph1	0.07216	Or1_ph2_pat1	0
Biso_V10_ph1	0.757	Z_O32_ph1	0.02455	Or2_ph2_pat1	0
Occ_V10_ph1	1	Biso_O32_ph1	1.689	Asym1_ph2_pat1	0
X_V11_ph1	0.30164	Occ_O32_ph1	1	Asym2_ph2_pat1	0
Y_V11_ph1	0.12878	X_O33_ph1	0.35597	Asym3_ph2_pat1	0
Z_V11_ph1	0.03361	Y_O33_ph1	0.27237	Asym4_ph2_pat1	0
Biso_V11_ph1	0.679	Z_O33_ph1	-0.03702	X_Zr1_ph2	0.2758

Occ_V11_ph1	1	Biso_O33_ph1	1.587	Y_Zr1_ph2	0.0411
X_V12_ph1	0.37478	Occ_O33_ph1	1	Z_Zr1_ph2	0.2082
Y_V12_ph1	0.21139	X_O34_ph1	0.43498	Biso_Zr1_ph2	0.303
Z_V12_ph1	-0.0395	Y_O34_ph1	0.20653	Occ_Zr1_ph2	1
Biso_V12_ph1	0.765	Z_O34_ph1	-0.01851	X_O2_ph2	0.0703
Occ_V12_ph1	1	Biso_O34_ph1	1.721	Y_O2_ph2	0.3359
X_V13_ph1	0.53727	Occ_O34_ph1	1	Z_O2_ph2	0.3406
Y_V13_ph1	0.54143	X_O35_ph1	0.37015	Biso_O2_ph2	0.316
Z_V13_ph1	0.20594	Y_O35_ph1	0.18931	Occ_O2_ph2	1
Biso_V13_ph1	0.757	Z_O35_ph1	-0.09934	X_O3_ph2	0.4423
Occ_V13_ph1	1	Biso_O35_ph1	1.808	Y_O3_ph2	0.7549
X_V14_ph1	0.53403	Occ_O35_ph1	1	Z_O3_ph2	0.4789
Y_V14_ph1	0.20035	X_O36_ph1	0.5206	Biso_O3_ph2	0.228
Occ_O3_ph2	1				

Phase Analysis Report.
Sample: sol-gel_160 °C

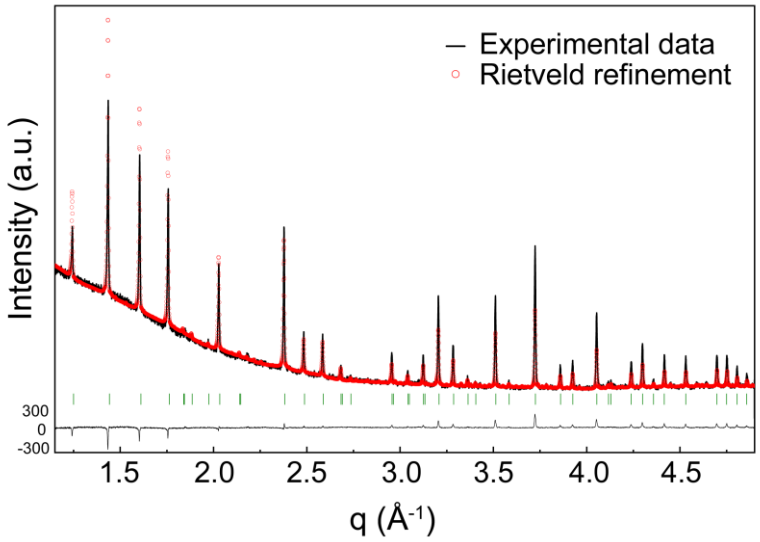

Figure S6. Rietveld refinement plot, showing the observed (black), calculated (red) and difference patterns of ZrV_2O_7 sol-gel_160 °C sample. Vertical lines indicate the positions of the Bragg reflections.

Sample and refinement data

Data range	16.149° - 75.234° 2Θ
Original data range	5.000° - 79.999°
Step size	0.009
Rietveld refinement converged	Yes
α2 subtracted	No
Background subtracted	No
Data smoothed	No
2theta correction	0.08346°
Radiation	X-rays
Method	Rietveld refinement
Automatic refinement	No
Final weighted average Bragg R factor	43.4
Final reduced chi^2	11.3

Matched phases

Amount (%)	Name	Formula sum	COD ID
100		O7 V2 Zr	2002983
2.7	Unidentified peak area		

Parameter List for Refinement

Parameter	Final value	Parameter	Final value	Parameter	Final value
Zero_pat1	0.0834608	Occ_V12_ph1	1	X_O32_ph1	0.32893
Lambda_pat1	1.54035	X_V13_ph1	0.53727	Y_O32_ph1	0.07216
Scale_ph1_pat1	1.99705E-07	Y_V13_ph1	0.54143	Z_O32_ph1	0.02455
Asym2_ph1_pat1	0.0427402	Z_V13_ph1	0.20594	Biso_O32_ph1	1.689
SyCos_pat1	0	Biso_V13_ph1	0.757	Occ_O32_ph1	1
SySin_pat1	0	Occ_V13_ph1	1	X_O33_ph1	0.35597
P0_mabs_pat1	0	X_V14_ph1	0.53403	Y_O33_ph1	0.27237
Cp_mabs_pat1	0	Y_V14_ph1	0.20035	Z_O33_ph1	-0.03702
Tau_mabs_pat1	0.1	Z_V14_ph1	0.21313	Biso_O33_ph1	1.587
Bck_0_pat1	1.00354	Biso_V14_ph1	0.726	Occ_O33_ph1	1
Bck_1_pat1	0	Occ_V14_ph1	1	X_O34_ph1	0.43498
Bck_2_pat1	0	X_V15_ph1	0.20147	Y_O34_ph1	0.20653
Bck_3_pat1	0	Y_V15_ph1	0.20147	Z_O34_ph1	-0.01851
Bover_ph1_pat1	0	Z_V15_ph1	0.20147	Biso_O34_ph1	1.721
Strain1_ph1_pat1	0	Biso_V15_ph1	0.813	Occ_O34_ph1	1
Strain2_ph1_pat1	0	Occ_V15_ph1	1	X_O35_ph1	0.37015
Strain3_ph1_pat1	0	X_V16_ph1	0.53834	Y_O35_ph1	0.18931
G-Size_ph1_pat1	0	Y_V16_ph1	0.53834	Z_O35_ph1	-0.09934
L-Size_ph1_pat1	0	Z_V16_ph1	0.53834	Biso_O35_ph1	1.808
Y-cos_ph1_pat1	0	Biso_V16_ph1	0.686	Occ_O35_ph1	1
EtaRght0_ph1_pat1	0	Occ_V16_ph1	1	X_O36_ph1	0.5206
X-tan_ph1_pat1	0	X_V17_ph1	0.12459	Y_O36_ph1	0.53508
U-Cagl_ph1_pat1	0	Y_V17_ph1	0.12459	Z_O36_ph1	0.26734
V-Cagl_ph1_pat1	0	Z_V17_ph1	0.12459	Biso_O36_ph1	1.744
W-Cagl_ph1_pat1	0.0105257	Biso_V17_ph1	0.734	Occ_O36_ph1	1
EtaPV_ph1_pat1	0.476126	Occ_V17_ph1	1	X_O37_ph1	0.51715
Cell_A_ph1_pat1	26.2788	X_O18_ph1	0.48004	Y_O37_ph1	0.59745
Cell_B_ph1_pat1	26.2788	Y_O18_ph1	0.06539	Z_O37_ph1	0.18395
Cell_C_ph1_pat1	26.2788	Z_O18_ph1	0.1262	Biso_O37_ph1	1.871
Cell_D_ph1_pat1	90	Biso_O18_ph1	1.523	Occ_O37_ph1	1
Cell_E_ph1_pat1	90	Occ_O18_ph1	1	X_O38_ph1	0.60074
Cell_F_ph1_pat1	90	X_O19_ph1	0.40009	Y_O38_ph1	0.53739
Or1_ph1_pat1	0	Y_O19_ph1	0.12892	Z_O38_ph1	0.20051
Or2_ph1_pat1	0	Z_O19_ph1	0.1466	Biso_O38_ph1	1.808
Asym1_ph1_pat1	0	Biso_O19_ph1	1.871	Occ_O38_ph1	1
Asym3_ph1_pat1	0	Occ_O19_ph1	1	X_O39_ph1	0.51072
Asym4_ph1_pat1	0	X_O20_ph1	0.47258	Y_O39_ph1	0.25854
X_Zr1_ph1	0.497434	Y_O20_ph1	0.15725	Z_O39_ph1	0.20207
Y_Zr1_ph1	-0.001114	Z_O20_ph1	0.07648	Biso_O39_ph1	1.823
Z_Zr1_ph1	0.165602	Biso_O20_ph1	1.555	Occ_O39_ph1	1
Biso_Zr1_ph1	0.497	Occ_O20_ph1	1	X_O40_ph1	0.59407
Occ_Zr1_ph1	1	X_O21_ph1	0.49048	Y_O40_ph1	0.19718
X_Zr2_ph1	0.500084	Y_O21_ph1	0.39627	Z_O40_ph1	0.19242
Y_Zr2_ph1	0.32661	Z_O21_ph1	0.12804	Biso_O40_ph1	1.808
Z_Zr2_ph1	0.164329	Biso_O21_ph1	1.618	Occ_O40_ph1	1
Biso_Zr2_ph1	0.481	Occ_O21_ph1	1	X_O41_ph1	0.5323
Occ_Zr2_ph1	1	X_O22_ph1	0.4726	Y_O41_ph1	0.18804
X_Zr3_ph1	0.496217	Y_O22_ph1	0.48128	Z_O41_ph1	0.2758

Y_Zr3_ph1	0.170143	Z_O22_ph1	0.07129	Biso_O41_ph1	1.847
Z_Zr3_ph1	0.34384	Biso_O22_ph1	1.823	Occ_O41_ph1	1
Biso_Zr3_ph1	0.426	Occ_O22_ph1	1	X_O42_ph1	0.26222
Occ_Zr3_ph1	1	X_O23_ph1	0.41032	Y_O42_ph1	0.1951
X_Zr4_ph1	0.331355	Y_O23_ph1	0.45904	Z_O42_ph1	0.18376
Y_Zr4_ph1	0.162024	Z_O23_ph1	0.15181	Biso_O42_ph1	1.958
Z_Zr4_ph1	0.166102	Biso_O23_ph1	1.594	Occ_O42_ph1	1
Biso_Zr4_ph1	0.505	Occ_O23_ph1	1	X_O43_ph1	0.59815
Occ_Zr4_ph1	1	X_O24_ph1	0.3524	Y_O43_ph1	-0.01624
X_Zr5_ph1	0.334645	Y_O24_ph1	0.3083	Z_O43_ph1	0.03707
Y_Zr5_ph1	0.334645	Z_O24_ph1	0.06917	Biso_O43_ph1	1.531
Z_Zr5_ph1	0.334645	Biso_O24_ph1	2.044	Occ_O43_ph1	1
Biso_Zr5_ph1	0.536	Occ_O24_ph1	1	X_O44_ph1	0.06452
Occ_Zr5_ph1	1	X_O25_ph1	0.3565	Y_O44_ph1	0.14578
X_Zr6_ph1	0	Y_O25_ph1	0.22994	Z_O44_ph1	0.12622
Y_Zr6_ph1	0	Z_O25_ph1	0.1359	Biso_O44_ph1	1.713
Z_Zr6_ph1	0	Biso_O25_ph1	2.218	Occ_O44_ph1	1
Biso_Zr6_ph1	0.505	Occ_O25_ph1	1	X_O45_ph1	0.4973
Occ_Zr6_ph1	1	X_O26_ph1	0.43193	Y_O45_ph1	0.155
X_V7_ph1	0.46207	Y_O26_ph1	0.3013	Z_O45_ph1	0.1807
Y_V7_ph1	0.12653	Z_O26_ph1	0.13571	Biso_O45_ph1	2.423
Z_V7_ph1	0.13145	Biso_O26_ph1	1.91	Occ_O45_ph1	1
Biso_V7_ph1	0.781	Occ_O26_ph1	1	X_O46_ph1	0.5101
Occ_V7_ph1	1	X_O27_ph1	0.23557	Y_O46_ph1	0.492
X_V8_ph1	0.4703	Y_O27_ph1	0.3606	Z_O46_ph1	0.1707
Y_V8_ph1	0.45683	Z_O27_ph1	0.18436	Biso_O46_ph1	2.55
Z_V8_ph1	0.12993	Biso_O27_ph1	1.879	Occ_O46_ph1	1
Biso_V8_ph1	0.742	Occ_O27_ph1	1	X_O47_ph1	0.3362
Occ_V8_ph1	1	X_O28_ph1	0.3133	Y_O47_ph1	0.3271
X_V9_ph1	0.36952	Y_O28_ph1	0.42848	Z_O47_ph1	0.173
Y_V9_ph1	0.29152	Z_O28_ph1	0.1951	Biso_O47_ph1	2.866
Z_V9_ph1	0.12774	Biso_O28_ph1	2.029	Occ_O47_ph1	1
Biso_V9_ph1	0.742	Occ_O28_ph1	1	X_O48_ph1	0.3357
Occ_V9_ph1	1	X_O29_ph1	0.29834	Y_O48_ph1	0.1759
X_V10_ph1	0.29521	Y_O29_ph1	0.35604	Z_O48_ph1	0.0004
Y_V10_ph1	0.36857	Z_O29_ph1	0.26787	Biso_O48_ph1	2.645
Z_V10_ph1	0.20539	Biso_O29_ph1	1.831	Occ_O48_ph1	1
Biso_V10_ph1	0.757	Occ_O29_ph1	1	X_O49_ph1	0.16284
Occ_V10_ph1	1	X_O30_ph1	0.3018	Y_O49_ph1	0.16284
X_V11_ph1	0.30164	Y_O30_ph1	0.14271	Z_O49_ph1	0.16284
Y_V11_ph1	0.12878	Z_O30_ph1	0.09573	Biso_O49_ph1	2.842
Z_V11_ph1	0.03361	Biso_O30_ph1	1.792	Occ_O49_ph1	1
Biso_V11_ph1	0.679	Occ_O30_ph1	1	X_O50_ph1	0.5
Occ_V11_ph1	1	X_O31_ph1	0.24174	Y_O50_ph1	0.5
X_V12_ph1	0.37478	Y_O31_ph1	0.12759	Z_O50_ph1	0.5
Y_V12_ph1	0.21139	Z_O31_ph1	0.01154	Biso_O50_ph1	2.85
Z_V12_ph1	-0.0395	Biso_O31_ph1	1.65	Occ_O50_ph1	1
Biso_V12_ph1	0.765	Occ_O31_ph1	1		

Sample: sol-gel_100 °C

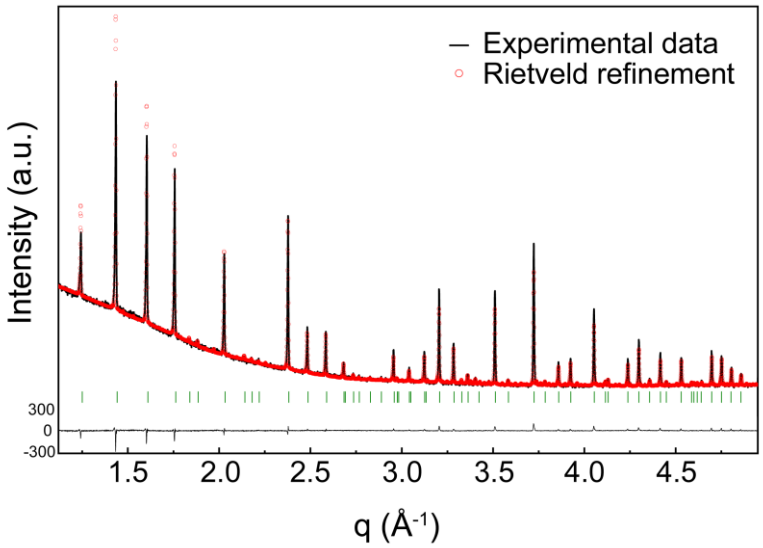

Figure S7. Rietveld refinement plot, showing the observed (black), calculated (red) and difference patterns of ZrV_2O_7 sol-gel_100 °C sample. Vertical lines indicate the positions of the Bragg reflections.

Sample and refinement data

Data range	15.764° - 75.200° 2Θ
Original data range	5.000° - 79.999°
Step size	0.009
Rietveld refinement converged	Yes
α2 subtracted	No
Background subtracted	No
Data smoothed	No
2theta correction	0.07834°
Radiation	X-rays
Method	Rietveld refinement
Automatic refinement	No
Final weighted average Bragg R factor	19.4
Final reduced chi^2	5.9

Matched phases

Amount (%)	Name	Formula sum	COD ID
100		O7 V2 Zr	2002983
1.8	Unidentified peak area		

Parameter List for Refinement

Parameter	Final value	Parameter	Final value	Parameter	Final value
Zero_pat1	0.0783446	Occ_V12_ph1	1	X_O32_ph1	0.32893
Lambda_pat1	1.53686	X_V13_ph1	0.53727	Y_O32_ph1	0.07216
Bck_0_pat1	0.986979	Y_V13_ph1	0.54143	Z_O32_ph1	0.02455
Scale_ph1_pat1	4.51303E-07	Z_V13_ph1	0.20594	Biso_O32_ph1	1.689
Cell_A_ph1_pat1	26.2248	Biso_V13_ph1	0.757	Occ_O32_ph1	1
Asym2_ph1_pat1	0.0472528	Occ_V13_ph1	1	X_O33_ph1	0.35597
SyCos_pat1	0	X_V14_ph1	0.53403	Y_O33_ph1	0.27237
SySin_pat1	0	Y_V14_ph1	0.20035	Z_O33_ph1	-0.03702
P0_mabs_pat1	0	Z_V14_ph1	0.21313	Biso_O33_ph1	1.587
Cp_mabs_pat1	0	Biso_V14_ph1	0.726	Occ_O33_ph1	1
Tau_mabs_pat1	0.1	Occ_V14_ph1	1	X_O34_ph1	0.43498
Bck_1_pat1	0	X_V15_ph1	0.20147	Y_O34_ph1	0.20653
Bck_2_pat1	0	Y_V15_ph1	0.20147	Z_O34_ph1	-0.01851
Bck_3_pat1	0	Z_V15_ph1	0.20147	Biso_O34_ph1	1.721
Bover_ph1_pat1	0	Biso_V15_ph1	0.813	Occ_O34_ph1	1
Strain1_ph1_pat1	0	Occ_V15_ph1	1	X_O35_ph1	0.37015
Strain2_ph1_pat1	0	X_V16_ph1	0.53834	Y_O35_ph1	0.18931
Strain3_ph1_pat1	0	Y_V16_ph1	0.53834	Z_O35_ph1	-0.09934
G-Size_ph1_pat1	0	Z_V16_ph1	0.53834	Biso_O35_ph1	1.808
L-Size_ph1_pat1	0	Biso_V16_ph1	0.686	Occ_O35_ph1	1
Y-cos_ph1_pat1	0	Occ_V16_ph1	1	X_O36_ph1	0.5206
EtaRght0_ph1_pat1	0	X_V17_ph1	0.12459	Y_O36_ph1	0.53508
X-tan_ph1_pat1	0	Y_V17_ph1	0.12459	Z_O36_ph1	0.26734
U-Cagl_ph1_pat1	0	Z_V17_ph1	0.12459	Biso_O36_ph1	1.744
V-Cagl_ph1_pat1	0	Biso_V17_ph1	0.734	Occ_O36_ph1	1
W-Cagl_ph1_pat1	0.00867596	Occ_V17_ph1	1	X_O37_ph1	0.51715
EtaPV_ph1_pat1	0.207288	X_O18_ph1	0.48004	Y_O37_ph1	0.59745
Cell_B_ph1_pat1	26.2245	Y_O18_ph1	0.06539	Z_O37_ph1	0.18395
Cell_C_ph1_pat1	26.2245	Z_O18_ph1	0.1262	Biso_O37_ph1	1.871
Cell_D_ph1_pat1	90	Biso_O18_ph1	1.523	Occ_O37_ph1	1
Cell_E_ph1_pat1	90	Occ_O18_ph1	1	X_O38_ph1	0.60074
Cell_F_ph1_pat1	90	X_O19_ph1	0.40009	Y_O38_ph1	0.53739
Or1_ph1_pat1	0	Y_O19_ph1	0.12892	Z_O38_ph1	0.20051
Or2_ph1_pat1	0	Z_O19_ph1	0.1466	Biso_O38_ph1	1.808
Asym1_ph1_pat1	0	Biso_O19_ph1	1.871	Occ_O38_ph1	1
Asym3_ph1_pat1	0	Occ_O19_ph1	1	X_O39_ph1	0.51072
Asym4_ph1_pat1	0	X_O20_ph1	0.47258	Y_O39_ph1	0.25854
X_Zr1_ph1	0.497434	Y_O20_ph1	0.15725	Z_O39_ph1	0.20207
Y_Zr1_ph1	-0.001114	Z_O20_ph1	0.07648	Biso_O39_ph1	1.823
Z_Zr1_ph1	0.165602	Biso_O20_ph1	1.555	Occ_O39_ph1	1
Biso_Zr1_ph1	0.497	Occ_O20_ph1	1	X_O40_ph1	0.59407
Occ_Zr1_ph1	1	X_O21_ph1	0.49048	Y_O40_ph1	0.19718
X_Zr2_ph1	0.500084	Y_O21_ph1	0.39627	Z_O40_ph1	0.19242
Y_Zr2_ph1	0.32661	Z_O21_ph1	0.12804	Biso_O40_ph1	1.808
Z_Zr2_ph1	0.164329	Biso_O21_ph1	1.618	Occ_O40_ph1	1
Biso_Zr2_ph1	0.481	Occ_O21_ph1	1	X_O41_ph1	0.5323
Occ_Zr2_ph1	1	X_O22_ph1	0.4726	Y_O41_ph1	0.18804
X_Zr3_ph1	0.496217	Y_O22_ph1	0.48128	Z_O41_ph1	0.2758

Y_Zr3_ph1	0.170143	Z_O22_ph1	0.07129	Biso_O41_ph1	1.847
Z_Zr3_ph1	0.34384	Biso_O22_ph1	1.823	Occ_O41_ph1	1
Biso_Zr3_ph1	0.426	Occ_O22_ph1	1	X_O42_ph1	0.26222
Occ_Zr3_ph1	1	X_O23_ph1	0.41032	Y_O42_ph1	0.1951
X_Zr4_ph1	0.331355	Y_O23_ph1	0.45904	Z_O42_ph1	0.18376
Y_Zr4_ph1	0.162024	Z_O23_ph1	0.15181	Biso_O42_ph1	1.958
Z_Zr4_ph1	0.166102	Biso_O23_ph1	1.594	Occ_O42_ph1	1
Biso_Zr4_ph1	0.505	Occ_O23_ph1	1	X_O43_ph1	0.59815
Occ_Zr4_ph1	1	X_O24_ph1	0.3524	Y_O43_ph1	-0.01624
X_Zr5_ph1	0.334645	Y_O24_ph1	0.3083	Z_O43_ph1	0.03707
Y_Zr5_ph1	0.334645	Z_O24_ph1	0.06917	Biso_O43_ph1	1.531
Z_Zr5_ph1	0.334645	Biso_O24_ph1	2.044	Occ_O43_ph1	1
Biso_Zr5_ph1	0.536	Occ_O24_ph1	1	X_O44_ph1	0.06452
Occ_Zr5_ph1	1	X_O25_ph1	0.3565	Y_O44_ph1	0.14578
X_Zr6_ph1	0	Y_O25_ph1	0.22994	Z_O44_ph1	0.12622
Y_Zr6_ph1	0	Z_O25_ph1	0.1359	Biso_O44_ph1	1.713
Z_Zr6_ph1	0	Biso_O25_ph1	2.218	Occ_O44_ph1	1
Biso_Zr6_ph1	0.505	Occ_O25_ph1	1	X_O45_ph1	0.4973
Occ_Zr6_ph1	1	X_O26_ph1	0.43193	Y_O45_ph1	0.155
X_V7_ph1	0.46207	Y_O26_ph1	0.3013	Z_O45_ph1	0.1807
Y_V7_ph1	0.12653	Z_O26_ph1	0.13571	Biso_O45_ph1	2.423
Z_V7_ph1	0.13145	Biso_O26_ph1	1.91	Occ_O45_ph1	1
Biso_V7_ph1	0.781	Occ_O26_ph1	1	X_O46_ph1	0.5101
Occ_V7_ph1	1	X_O27_ph1	0.23557	Y_O46_ph1	0.492
X_V8_ph1	0.4703	Y_O27_ph1	0.3606	Z_O46_ph1	0.1707
Y_V8_ph1	0.45683	Z_O27_ph1	0.18436	Biso_O46_ph1	2.55
Z_V8_ph1	0.12993	Biso_O27_ph1	1.879	Occ_O46_ph1	1
Biso_V8_ph1	0.742	Occ_O27_ph1	1	X_O47_ph1	0.3362
Occ_V8_ph1	1	X_O28_ph1	0.3133	Y_O47_ph1	0.3271
X_V9_ph1	0.36952	Y_O28_ph1	0.42848	Z_O47_ph1	0.173
Y_V9_ph1	0.29152	Z_O28_ph1	0.1951	Biso_O47_ph1	2.866
Z_V9_ph1	0.12774	Biso_O28_ph1	2.029	Occ_O47_ph1	1
Biso_V9_ph1	0.742	Occ_O28_ph1	1	X_O48_ph1	0.3357
Occ_V9_ph1	1	X_O29_ph1	0.29834	Y_O48_ph1	0.1759
X_V10_ph1	0.29521	Y_O29_ph1	0.35604	Z_O48_ph1	0.0004
Y_V10_ph1	0.36857	Z_O29_ph1	0.26787	Biso_O48_ph1	2.645
Z_V10_ph1	0.20539	Biso_O29_ph1	1.831	Occ_O48_ph1	1
Biso_V10_ph1	0.757	Occ_O29_ph1	1	X_O49_ph1	0.16284
Occ_V10_ph1	1	X_O30_ph1	0.3018	Y_O49_ph1	0.16284
X_V11_ph1	0.30164	Y_O30_ph1	0.14271	Z_O49_ph1	0.16284
Y_V11_ph1	0.12878	Z_O30_ph1	0.09573	Biso_O49_ph1	2.842
Z_V11_ph1	0.03361	Biso_O30_ph1	1.792	Occ_O49_ph1	1
Biso_V11_ph1	0.679	Occ_O30_ph1	1	X_O50_ph1	0.5
Occ_V11_ph1	1	X_O31_ph1	0.24174	Y_O50_ph1	0.5
X_V12_ph1	0.37478	Y_O31_ph1	0.12759	Z_O50_ph1	0.5
Y_V12_ph1	0.21139	Z_O31_ph1	0.01154	Biso_O50_ph1	2.85
Z_V12_ph1	-0.0395	Biso_O31_ph1	1.65	Occ_O50_ph1	1
Biso_V12_ph1	0.765	Occ_O31_ph1	1		

Sample: sol-gel_RO^-

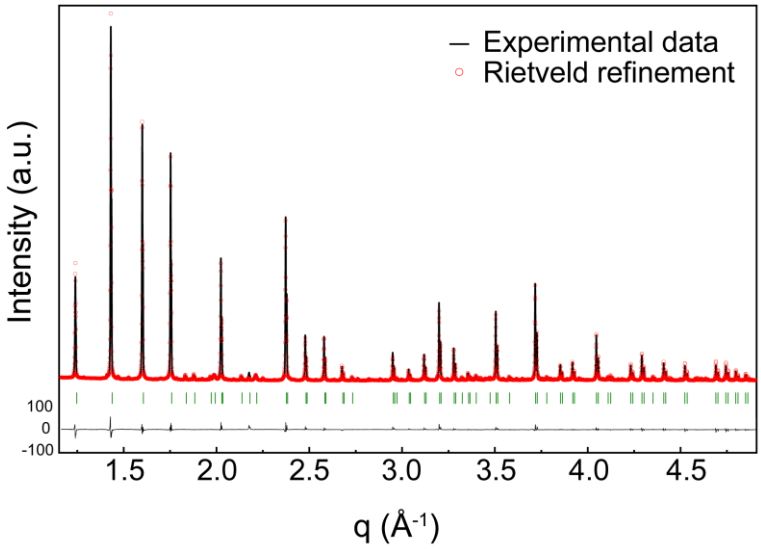

Figure S8. Rietveld refinement plot, showing the observed (black), calculated (red) and difference patterns of ZrV_2O_7 sol-gel_RO^- sample. Vertical lines indicate the positions of the Bragg reflections.

Sample and refinement data

Data range	16.417° - 74.822° 2Θ
Original data range	5.000° - 99.985°
Step size	0.010
Rietveld refinement converged	Yes
α2 subtracted	No
Background subtracted	No
Data smoothed	No
Specimen displacement correction (Bragg-Brentano geometry)	T = (-s/R) = 0.00034842
Radiation	X-rays
Method	Rietveld refinement
Automatic refinement	No
Final weighted average Bragg R factor	5.2
Final reduced chi^2	12.0

Matched phases

Amount (%)	Name	Formula sum	COD ID
97.1		O7 V2 Zr	2002983
2.9	Baddeleyite	O2 Zr	9007485
3.6	Unidentified peak area		

Parameter List for Refinement

Parameter	Final value	Parameter	Final value	Parameter	Final value
SyCos_pat1	0.0399265	Z_V14_ph1	0.21313	Y_O36_ph1	0.53508
Bck_0_pat1	1.00027	Biso_V14_ph1	0.726	Z_O36_ph1	0.26734
Scale_ph1_pat1	1.32634E-06	Occ_V14_ph1	1	Biso_O36_ph1	1.744
X-tan_ph1_pat1	0.00681974	X_V15_ph1	0.20147	Occ_O36_ph1	1
W-Cagl_ph1_pat1	0.00267654	Y_V15_ph1	0.20147	X_O37_ph1	0.51715
EtaPV_ph1_pat1	0.353666	Z_V15_ph1	0.20147	Y_O37_ph1	0.59745

Cell_A_ph1_pat1	26.3265	Biso_V15_ph1	0.813	Z_O37_ph1	0.18395
Scale_ph2_pat1	0.000339289	Occ_V15_ph1	1	Biso_O37_ph1	1.871
Cell_A_ph2_pat1	5.14302	X_V16_ph1	0.53834	Occ_O37_ph1	1
Cell_B_ph2_pat1	5.1998	Y_V16_ph1	0.53834	X_O38_ph1	0.60074
Cell_C_ph2_pat1	5.3196	Z_V16_ph1	0.53834	Y_O38_ph1	0.53739
Cell_E_ph2_pat1	99.1168	Biso_V16_ph1	0.686	Z_O38_ph1	0.20051
Zero_pat1	0	Occ_V16_ph1	1	Biso_O38_ph1	1.808
SySin_pat1	0	X_V17_ph1	0.12459	Occ_O38_ph1	1
Lambda_pat1	1.54187	Y_V17_ph1	0.12459	X_O39_ph1	0.51072
P0_mabs_pat1	0	Z_V17_ph1	0.12459	Y_O39_ph1	0.25854
Cp_mabs_pat1	0	Biso_V17_ph1	0.734	Z_O39_ph1	0.20207
Tau_mabs_pat1	0.1	Occ_V17_ph1	1	Biso_O39_ph1	1.823
Bck_1_pat1	0	X_O18_ph1	0.48004	Occ_O39_ph1	1
Bck_2_pat1	0	Y_O18_ph1	0.06539	X_O40_ph1	0.59407
Bck_3_pat1	0	Z_O18_ph1	0.1262	Y_O40_ph1	0.19718
Bover_ph1_pat1	0	Biso_O18_ph1	1.523	Z_O40_ph1	0.19242
Strain1_ph1_pat1	0	Occ_O18_ph1	1	Biso_O40_ph1	1.808
Strain2_ph1_pat1	0	X_O19_ph1	0.40009	Occ_O40_ph1	1
Strain3_ph1_pat1	0	Y_O19_ph1	0.12892	X_O41_ph1	0.5323
G-Size_ph1_pat1	0	Z_O19_ph1	0.1466	Y_O41_ph1	0.18804
L-Size_ph1_pat1	0	Biso_O19_ph1	1.871	Z_O41_ph1	0.2758
Y-cos_ph1_pat1	0	Occ_O19_ph1	1	Biso_O41_ph1	1.847
EtaRght0_ph1_pat1	0	X_O20_ph1	0.47258	Occ_O41_ph1	1
U-Cagl_ph1_pat1	0	Y_O20_ph1	0.15725	X_O42_ph1	0.26222
V-Cagl_ph1_pat1	0	Z_O20_ph1	0.07648	Y_O42_ph1	0.1951
Cell_B_ph1_pat1	26.3264	Biso_O20_ph1	1.555	Z_O42_ph1	0.18376
Cell_C_ph1_pat1	26.3264	Occ_O20_ph1	1	Biso_O42_ph1	1.958
Cell_D_ph1_pat1	90	X_O21_ph1	0.49048	Occ_O42_ph1	1
Cell_E_ph1_pat1	90	Y_O21_ph1	0.39627	X_O43_ph1	0.59815
Cell_F_ph1_pat1	90	Z_O21_ph1	0.12804	Y_O43_ph1	-0.01624
Or1_ph1_pat1	0	Biso_O21_ph1	1.618	Z_O43_ph1	0.03707
Or2_ph1_pat1	0	Occ_O21_ph1	1	Biso_O43_ph1	1.531
Asym1_ph1_pat1	0	X_O22_ph1	0.4726	Occ_O43_ph1	1
Asym2_ph1_pat1	0.0283191	Y_O22_ph1	0.48128	X_O44_ph1	0.06452
Asym3_ph1_pat1	0	Z_O22_ph1	0.07129	Y_O44_ph1	0.14578
Asym4_ph1_pat1	0	Biso_O22_ph1	1.823	Z_O44_ph1	0.12622
X_Zr1_ph1	0.497434	Occ_O22_ph1	1	Biso_O44_ph1	1.713
Y_Zr1_ph1	-0.001114	X_O23_ph1	0.41032	Occ_O44_ph1	1
Z_Zr1_ph1	0.165602	Y_O23_ph1	0.45904	X_O45_ph1	0.4973
Biso_Zr1_ph1	0.497	Z_O23_ph1	0.15181	Y_O45_ph1	0.155
Occ_Zr1_ph1	1	Biso_O23_ph1	1.594	Z_O45_ph1	0.1807
X_Zr2_ph1	0.500084	Occ_O23_ph1	1	Biso_O45_ph1	2.423
Y_Zr2_ph1	0.32661	X_O24_ph1	0.3524	Occ_O45_ph1	1
Z_Zr2_ph1	0.164329	Y_O24_ph1	0.3083	X_O46_ph1	0.5101
Biso_Zr2_ph1	0.481	Z_O24_ph1	0.06917	Y_O46_ph1	0.492
Occ_Zr2_ph1	1	Biso_O24_ph1	2.044	Z_O46_ph1	0.1707
X_Zr3_ph1	0.496217	Occ_O24_ph1	1	Biso_O46_ph1	2.55
Y_Zr3_ph1	0.170143	X_O25_ph1	0.3565	Occ_O46_ph1	1
Z_Zr3_ph1	0.34384	Y_O25_ph1	0.22994	X_O47_ph1	0.3362
Biso_Zr3_ph1	0.426	Z_O25_ph1	0.1359	Y_O47_ph1	0.3271

Occ_Zr3_ph1	1	Biso_O25_ph1	2.218	Z_O47_ph1	0.173
X_Zr4_ph1	0.331355	Occ_O25_ph1	1	Biso_O47_ph1	2.866
Y_Zr4_ph1	0.162024	X_O26_ph1	0.43193	Occ_O47_ph1	1
Z_Zr4_ph1	0.166102	Y_O26_ph1	0.3013	X_O48_ph1	0.3357
Biso_Zr4_ph1	0.505	Z_O26_ph1	0.13571	Y_O48_ph1	0.1759
Occ_Zr4_ph1	1	Biso_O26_ph1	1.91	Z_O48_ph1	0.0004
X_Zr5_ph1	0.334645	Occ_O26_ph1	1	Biso_O48_ph1	2.645
Y_Zr5_ph1	0.334645	X_O27_ph1	0.23557	Occ_O48_ph1	1
Z_Zr5_ph1	0.334645	Y_O27_ph1	0.3606	X_O49_ph1	0.16284
Biso_Zr5_ph1	0.536	Z_O27_ph1	0.18436	Y_O49_ph1	0.16284
Occ_Zr5_ph1	1	Biso_O27_ph1	1.879	Z_O49_ph1	0.16284
X_Zr6_ph1	0	Occ_O27_ph1	1	Biso_O49_ph1	2.842
Y_Zr6_ph1	0	X_O28_ph1	0.3133	Occ_O49_ph1	1
Z_Zr6_ph1	0	Y_O28_ph1	0.42848	X_O50_ph1	0.5
Biso_Zr6_ph1	0.505	Z_O28_ph1	0.1951	Y_O50_ph1	0.5
Occ_Zr6_ph1	1	Biso_O28_ph1	2.029	Z_O50_ph1	0.5
X_V7_ph1	0.46207	Occ_O28_ph1	1	Biso_O50_ph1	2.85
Y_V7_ph1	0.12653	X_O29_ph1	0.29834	Occ_O50_ph1	1
Z_V7_ph1	0.13145	Y_O29_ph1	0.35604	Bover_ph2_pat1	0
Biso_V7_ph1	0.781	Z_O29_ph1	0.26787	Strain1_ph2_pat1	0
Occ_V7_ph1	1	Biso_O29_ph1	1.831	Strain2_ph2_pat1	0
X_V8_ph1	0.4703	Occ_O29_ph1	1	Strain3_ph2_pat1	0
Y_V8_ph1	0.45683	X_O30_ph1	0.3018	G-Size_ph2_pat1	0
Z_V8_ph1	0.12993	Y_O30_ph1	0.14271	L-Size_ph2_pat1	0
Biso_V8_ph1	0.742	Z_O30_ph1	0.09573	Y-cos_ph2_pat1	0
Occ_V8_ph1	1	Biso_O30_ph1	1.792	X-tan_ph2_pat1	0.0132543
X_V9_ph1	0.36952	Occ_O30_ph1	1	U-Cagl_ph2_pat1	0
Y_V9_ph1	0.29152	X_O31_ph1	0.24174	V-Cagl_ph2_pat1	0
Z_V9_ph1	0.12774	Y_O31_ph1	0.12759	W-Cagl_ph2_pat1	0.037521
Biso_V9_ph1	0.742	Z_O31_ph1	0.01154	EtaPV_ph2_pat1	0.06132
Occ_V9_ph1	1	Biso_O31_ph1	1.65	Cell_D_ph2_pat1	90
X_V10_ph1	0.29521	Occ_O31_ph1	1	Cell_F_ph2_pat1	90
Y_V10_ph1	0.36857	X_O32_ph1	0.32893	Or1_ph2_pat1	0
Z_V10_ph1	0.20539	Y_O32_ph1	0.07216	Or2_ph2_pat1	0
Biso_V10_ph1	0.757	Z_O32_ph1	0.02455	Asym1_ph2_pat1	0
Occ_V10_ph1	1	Biso_O32_ph1	1.689	Asym2_ph2_pat1	0
X_V11_ph1	0.30164	Occ_O32_ph1	1	Asym3_ph2_pat1	0
Y_V11_ph1	0.12878	X_O33_ph1	0.35597	Asym4_ph2_pat1	0
Z_V11_ph1	0.03361	Y_O33_ph1	0.27237	X_Zr1_ph2	0.2758
Biso_V11_ph1	0.679	Z_O33_ph1	-0.03702	Y_Zr1_ph2	0.0411
Occ_V11_ph1	1	Biso_O33_ph1	1.587	Z_Zr1_ph2	0.2082
X_V12_ph1	0.37478	Occ_O33_ph1	1	Biso_Zr1_ph2	0.303
Y_V12_ph1	0.21139	X_O34_ph1	0.43498	Occ_Zr1_ph2	1
Z_V12_ph1	-0.0395	Y_O34_ph1	0.20653	X_O2_ph2	0.0703
Biso_V12_ph1	0.765	Z_O34_ph1	-0.01851	Y_O2_ph2	0.3359
Occ_V12_ph1	1	Biso_O34_ph1	1.721	Z_O2_ph2	0.3406
X_V13_ph1	0.53727	Occ_O34_ph1	1	Biso_O2_ph2	0.316
Y_V13_ph1	0.54143	X_O35_ph1	0.37015	Occ_O2_ph2	1
Z_V13_ph1	0.20594	Y_O35_ph1	0.18931	X_O3_ph2	0.4423
Biso_V13_ph1	0.757	Z_O35_ph1	-0.09934	Y_O3_ph2	0.7549

Occ_V13_ph1	1	Biso_O35_ph1	1.808	Z_O3_ph2	0.4789
X_V14_ph1	0.53403	Occ_O35_ph1	1	Biso_O3_ph2	0.228
Y_V14_ph1	0.20035	X_O36_ph1	0.5206	Occ_O3_ph2	1

Phase Analysis Report.
Sample: sol-gel_Cl

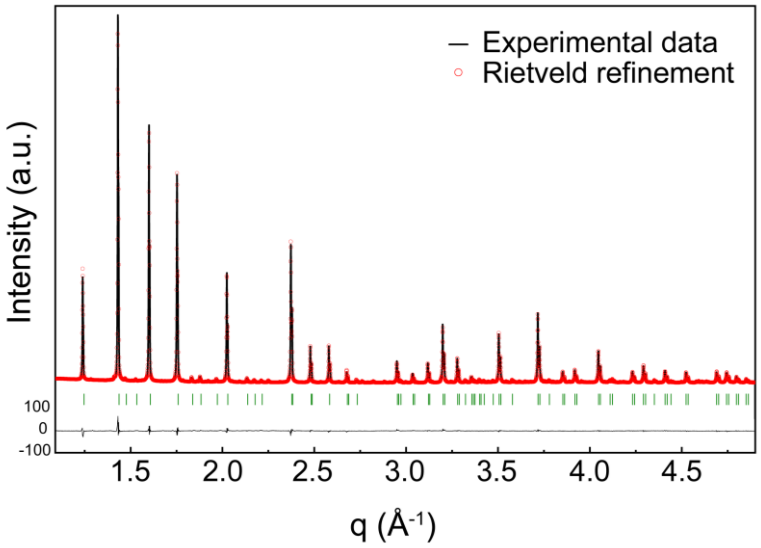

Figure S9. Rietveld refinement plot, showing the observed (black), calculated (red) and difference patterns of ZrV_2O_7 sol-gel_Cl sample. Vertical lines indicate the positions of the Bragg reflections.

Sample and refinement data

Data range	15.423° - 75.053° 2Θ
Original data range	5.000° - 99.985°
Step size	0.010
Rietveld refinement converged	Yes
α2 subtracted	No
Background subtracted	No
Data smoothed	No
Specimen displacement correction (Bragg-Brentano geometry)	T = (-s/R) = 0.00028593
Radiation	X-rays
Method	Rietveld refinement
Automatic refinement	No
Final weighted average Bragg R factor	4.6
Final reduced chi^2	8.4

Matched phases

Amount (%)	Name	Formula sum	COD ID
100		O7 V2 Zr	2002983
3.0	Unidentified peak area		

Parameter List for Refinement

Parameter	Final value	Parameter	Final value	Parameter	Final value
SyCos_pat1	0.0327651	Occ_V12_ph1	1	X_O32_ph1	0.32893
Bck_0_pat1	0.785282	X_V13_ph1	0.53727	Y_O32_ph1	0.07216
Bck_1_pat1	183.653	Y_V13_ph1	0.54143	Z_O32_ph1	0.02455
Bck_2_pat1	-0.0289183	Z_V13_ph1	0.20594	Biso_O32_ph1	1.689
Bck_3_pat1	1.77543	Biso_V13_ph1	0.757	Occ_O32_ph1	1
Scale_ph1_pat1	1.33317E-06	Occ_V13_ph1	1	X_O33_ph1	0.35597
X-tan_ph1_pat1	0.0101414	X_V14_ph1	0.53403	Y_O33_ph1	0.27237
U-Cagl_ph1_pat1	0.0129125	Y_V14_ph1	0.20035	Z_O33_ph1	-0.03702
V-Cagl_ph1_pat1	-0.00415464	Z_V14_ph1	0.21313	Biso_O33_ph1	1.587
W-Cagl_ph1_pat1	0.00367856	Biso_V14_ph1	0.726	Occ_O33_ph1	1
EtaPV_ph1_pat1	0.285648	Occ_V14_ph1	1	X_O34_ph1	0.43498
Cell_A_ph1_pat1	26.3282	X_V15_ph1	0.20147	Y_O34_ph1	0.20653
Asym2_ph1_pat1	0.0269896	Y_V15_ph1	0.20147	Z_O34_ph1	-0.01851
Zero_pat1	0	Z_V15_ph1	0.20147	Biso_O34_ph1	1.721
SySin_pat1	0	Biso_V15_ph1	0.813	Occ_O34_ph1	1
Lambda_pat1	1.54187	Occ_V15_ph1	1	X_O35_ph1	0.37015
P0_mabs_pat1	0	X_V16_ph1	0.53834	Y_O35_ph1	0.18931
Cp_mabs_pat1	0	Y_V16_ph1	0.53834	Z_O35_ph1	-0.09934
Tau_mabs_pat1	0.1	Z_V16_ph1	0.53834	Biso_O35_ph1	1.808
Bover_ph1_pat1	0	Biso_V16_ph1	0.686	Occ_O35_ph1	1
Strain1_ph1_pat1	0	Occ_V16_ph1	1	X_O36_ph1	0.5206
Strain2_ph1_pat1	0	X_V17_ph1	0.12459	Y_O36_ph1	0.53508
Strain3_ph1_pat1	0	Y_V17_ph1	0.12459	Z_O36_ph1	0.26734
G-Size_ph1_pat1	0	Z_V17_ph1	0.12459	Biso_O36_ph1	1.744
L-Size_ph1_pat1	0	Biso_V17_ph1	0.734	Occ_O36_ph1	1
Y-cos_ph1_pat1	0	Occ_V17_ph1	1	X_O37_ph1	0.51715
EtaRght0_ph1_pat1	0	X_O18_ph1	0.48004	Y_O37_ph1	0.59745
Cell_B_ph1_pat1	26.3274	Y_O18_ph1	0.06539	Z_O37_ph1	0.18395
Cell_C_ph1_pat1	26.3274	Z_O18_ph1	0.1262	Biso_O37_ph1	1.871
Cell_D_ph1_pat1	90	Biso_O18_ph1	1.523	Occ_O37_ph1	1
Cell_E_ph1_pat1	90	Occ_O18_ph1	1	X_O38_ph1	0.60074
Cell_F_ph1_pat1	90	X_O19_ph1	0.40009	Y_O38_ph1	0.53739
Or1_ph1_pat1	0	Y_O19_ph1	0.12892	Z_O38_ph1	0.20051
Or2_ph1_pat1	0	Z_O19_ph1	0.1466	Biso_O38_ph1	1.808
Asym1_ph1_pat1	0	Biso_O19_ph1	1.871	Occ_O38_ph1	1
Asym3_ph1_pat1	0	Occ_O19_ph1	1	X_O39_ph1	0.51072
Asym4_ph1_pat1	0	X_O20_ph1	0.47258	Y_O39_ph1	0.25854
X_Zr1_ph1	0.497434	Y_O20_ph1	0.15725	Z_O39_ph1	0.20207
Y_Zr1_ph1	-0.001114	Z_O20_ph1	0.07648	Biso_O39_ph1	1.823
Z_Zr1_ph1	0.165602	Biso_O20_ph1	1.555	Occ_O39_ph1	1
Biso_Zr1_ph1	0.497	Occ_O20_ph1	1	X_O40_ph1	0.59407
Occ_Zr1_ph1	1	X_O21_ph1	0.49048	Y_O40_ph1	0.19718
X_Zr2_ph1	0.500084	Y_O21_ph1	0.39627	Z_O40_ph1	0.19242
Y_Zr2_ph1	0.32661	Z_O21_ph1	0.12804	Biso_O40_ph1	1.808
Z_Zr2_ph1	0.164329	Biso_O21_ph1	1.618	Occ_O40_ph1	1
Biso_Zr2_ph1	0.481	Occ_O21_ph1	1	X_O41_ph1	0.5323
Occ_Zr2_ph1	1	X_O22_ph1	0.4726	Y_O41_ph1	0.18804
X_Zr3_ph1	0.496217	Y_O22_ph1	0.48128	Z_O41_ph1	0.2758
Y_Zr3_ph1	0.170143	Z_O22_ph1	0.07129	Biso_O41_ph1	1.847
Z_Zr3_ph1	0.34384	Biso_O22_ph1	1.823	Occ_O41_ph1	1
Biso_Zr3_ph1	0.426	Occ_O22_ph1	1	X_O42_ph1	0.26222
Occ_Zr3_ph1	1	X_O23_ph1	0.41032	Y_O42_ph1	0.1951
X_Zr4_ph1	0.331355	Y_O23_ph1	0.45904	Z_O42_ph1	0.18376
Y_Zr4_ph1	0.162024	Z_O23_ph1	0.15181	Biso_O42_ph1	1.958
Z_Zr4_ph1	0.166102	Biso_O23_ph1	1.594	Occ_O42_ph1	1
Biso_Zr4_ph1	0.505	Occ_O23_ph1	1	X_O43_ph1	0.59815
Occ_Zr4_ph1	1	X_O24_ph1	0.3524	Y_O43_ph1	-0.01624
X_Zr5_ph1	0.334645	Y_O24_ph1	0.3083	Z_O43_ph1	0.03707

Y_Zr5_ph1	0.334645	Z_O24_ph1	0.06917	Biso_O43_ph1	1.531
Z_Zr5_ph1	0.334645	Biso_O24_ph1	2.044	Occ_O43_ph1	1
Biso_Zr5_ph1	0.536	Occ_O24_ph1	1	X_O44_ph1	0.06452
Occ_Zr5_ph1	1	X_O25_ph1	0.3565	Y_O44_ph1	0.14578
X_Zr6_ph1	0	Y_O25_ph1	0.22994	Z_O44_ph1	0.12622
Y_Zr6_ph1	0	Z_O25_ph1	0.1359	Biso_O44_ph1	1.713
Z_Zr6_ph1	0	Biso_O25_ph1	2.218	Occ_O44_ph1	1
Biso_Zr6_ph1	0.505	Occ_O25_ph1	1	X_O45_ph1	0.4973
Occ_Zr6_ph1	1	X_O26_ph1	0.43193	Y_O45_ph1	0.155
X_V7_ph1	0.46207	Y_O26_ph1	0.3013	Z_O45_ph1	0.1807
Y_V7_ph1	0.12653	Z_O26_ph1	0.13571	Biso_O45_ph1	2.423
Z_V7_ph1	0.13145	Biso_O26_ph1	1.91	Occ_O45_ph1	1
Biso_V7_ph1	0.781	Occ_O26_ph1	1	X_O46_ph1	0.5101
Occ_V7_ph1	1	X_O27_ph1	0.23557	Y_O46_ph1	0.492
X_V8_ph1	0.4703	Y_O27_ph1	0.3606	Z_O46_ph1	0.1707
Y_V8_ph1	0.45683	Z_O27_ph1	0.18436	Biso_O46_ph1	2.55
Z_V8_ph1	0.12993	Biso_O27_ph1	1.879	Occ_O46_ph1	1
Biso_V8_ph1	0.742	Occ_O27_ph1	1	X_O47_ph1	0.3362
Occ_V8_ph1	1	X_O28_ph1	0.3133	Y_O47_ph1	0.3271
X_V9_ph1	0.36952	Y_O28_ph1	0.42848	Z_O47_ph1	0.173
Y_V9_ph1	0.29152	Z_O28_ph1	0.1951	Biso_O47_ph1	2.866
Z_V9_ph1	0.12774	Biso_O28_ph1	2.029	Occ_O47_ph1	1
Biso_V9_ph1	0.742	Occ_O28_ph1	1	X_O48_ph1	0.3357
Occ_V9_ph1	1	X_O29_ph1	0.29834	Y_O48_ph1	0.1759
X_V10_ph1	0.29521	Y_O29_ph1	0.35604	Z_O48_ph1	0.0004
Y_V10_ph1	0.36857	Z_O29_ph1	0.26787	Biso_O48_ph1	2.645
Z_V10_ph1	0.20539	Biso_O29_ph1	1.831	Occ_O48_ph1	1
Biso_V10_ph1	0.757	Occ_O29_ph1	1	X_O49_ph1	0.16284
Occ_V10_ph1	1	X_O30_ph1	0.3018	Y_O49_ph1	0.16284
X_V11_ph1	0.30164	Y_O30_ph1	0.14271	Z_O49_ph1	0.16284
Y_V11_ph1	0.12878	Z_O30_ph1	0.09573	Biso_O49_ph1	2.842
Z_V11_ph1	0.03361	Biso_O30_ph1	1.792	Occ_O49_ph1	1
Biso_V11_ph1	0.679	Occ_O30_ph1	1	X_O50_ph1	0.5
Occ_V11_ph1	1	X_O31_ph1	0.24174	Y_O50_ph1	0.5
X_V12_ph1	0.37478	Y_O31_ph1	0.12759	Z_O50_ph1	0.5
Y_V12_ph1	0.21139	Z_O31_ph1	0.01154	Biso_O50_ph1	2.85
Z_V12_ph1	-0.0395	Biso_O31_ph1	1.65	Occ_O50_ph1	1
Biso_V12_ph1	0.765	Occ_O31_ph1	1		

Raman spectroscopy

Experimental analysis

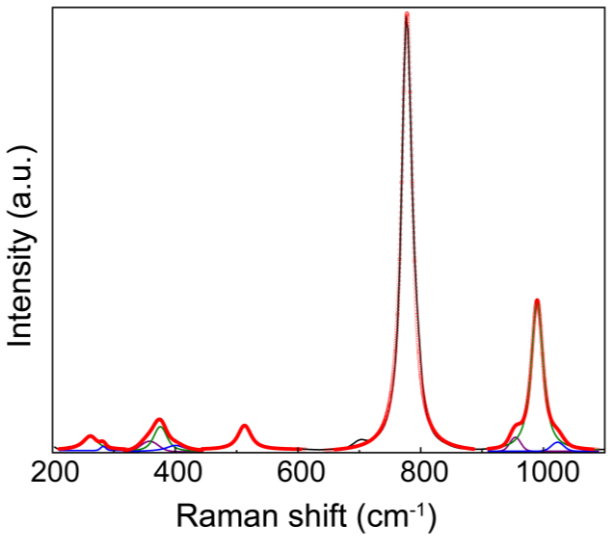

Figure S10. Fitted experimental Raman spectrum of sol-gel_100 °C sample at room temperature.

Table S2. A comparison of calculated frequencies with those obtained from fitting the experimental spectra. The Raman band positions were determined by peak fitting of the averaged spectra with the Voigt model. The frequency difference is defined as:

$\Delta\omega = |\omega_{fit} - \omega_{calc}|$.

Values marked in green were evaluated to fit best with the experimental spectra.

Experimental fitted peak position, (cm^{-1})	Calculated peak position, (cm^{-1})	$\Delta\omega = \|\omega_{fit} - \omega_{calc}\|$, ($cm^{-1}$)
261.8 ± 0.75	254.48	7.3
	262.66	0.9
358 ± 11.9	348.48	10
376 ± 1.6	366.16	10
400 ± 9.0	384.91	15
513.1 ± 0.19	492.88	20.2
	497.35	15.8
777.79 ± 0.091	798.75	20.96
	812.48	34.69
954.3 ± 0.16	967.20	12.9
989.93 ± 0.015	1004.46	14.53
1023.1 ± 0.29	1036.49	13.4

Computational simulations

The total energy was strictly converged using a Γ-centre grid of (6×6×6) k-points and ΔE < 10^{-8} and ΔE < 10^{-6} eV for the electronic and structural optimisation, respectively. A supercell approach in the framework of the finite displacement method, as implemented in Phonopy[3,4], was used to compute the harmonic vibrational properties of the material. A supercell of (3×3×3) with displacements of 0.01 Å was used to extract the harmonic force constants. The corresponding force calculations were done at Γ-point. Finally, to correct long-ranging dipole-dipole interaction, Born effective charge computations were also performed, and the non-analytical term correction as implemented in

Phonopy was applied[5,6]. After determining phonon eigenvectors and frequencies, Raman-active modes were extracted with Phonopy at the Gamma point by analysing the irreducible representations. A given mode is Raman-active if its irreducible representation (irrep) basis functions are quadratic (*xy*, x^2 etc.). This data was taken from the Bilbao Crystallographic Server point group tables.

GIFs of Raman active phonon vibrations were created using the phonon website, where computed atomic vibrations according to particular phonon modes can be visualised:

https://henriquemiranda.github.io/phononwebsite/phonon.html

The complete dataset, including visualization of phonon vibrations, is available at DOI: 10.5281/zenodo.12688634.[7]

Scanning electron microscopy (SEM)

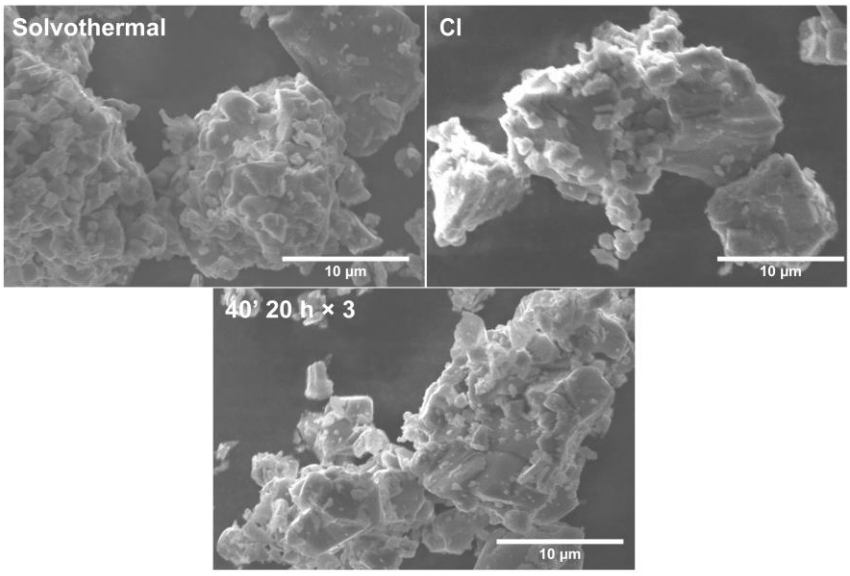

Figure S11. SEM images of solvothermal (top left), sol-gel_Cl (top right) and solid state 40' 20 h × 3 reactions. All samples show similar morphology.

Thermogravimetric analysis (TGA)

Method

Thermogravimetric analysis (TGA) was performed in a combined mode on dry powder using a heat flux TGA/DSC 3+ device from Mettler Toledo. All measurements were carried out under an air atmosphere (flow of 80 ml·min^{-1}). As a reference material for the heat flux DSC, an Al_2O_3 crucible was used. Samples were heated from room temperature to 400 or 700 °C with a heating rate of 10 °C min^{-1} and held for 20 h.

Results

To address the possible loss of V_2O_5 due to a higher volatilization ratio, we performed TGA measurements that would simulate the synthesis environment. We used a 40'-milled ZrO_2 and V_2O_5 mixture that was heated to 400 °C and 700 °C and held at the corresponding temperature for 20 h (see Figure S12).

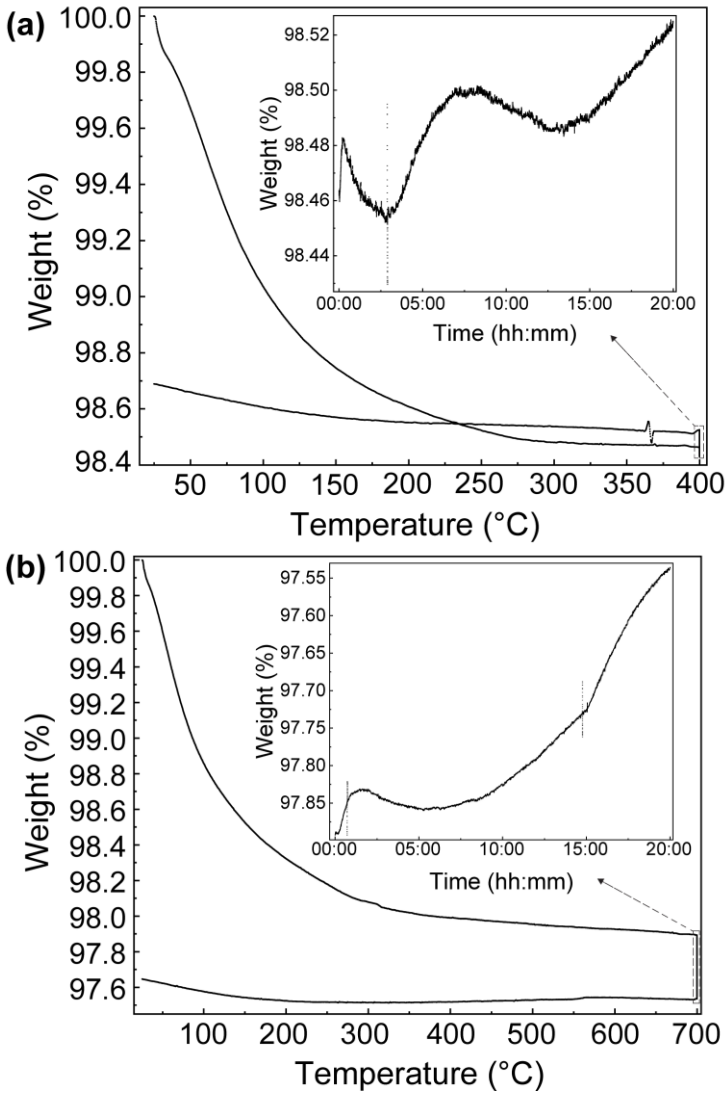

Figure S12. TGA of 40' milled ZrO_2 and V_2O_5 mixture heated from room temperature to 400 °C (a) and 700 °C (b) at 10 °C/min rate, held at that temperature for 20 h and cooled down to room temperature at 10 °C/min. Insets show corresponding weight change when holding for 20 h.

The total weight loss was barely 2.4% for the sample heated to 700 °C and 1.3% for the sample heated to 400 °C. We observed the highest decrease in weight % far below an expected V_2O_5 sublimation temperature. This loss is most likely attributed to the loss of ethanol and acetic acid (present in the sample due to ethanol grinding media that was used to combine starting oxides). We hypothesize that acetic acid, which was detected after milling experiments, was produced due to ethanol oxidation likely catalysed by the presence of ceramic powders and undergoing mechanochemical reaction. The ethanol evaporation temperature is 78 °C, while the boiling point of acetic acid reaches 118 °C. The sample heated up to 400 °C did not lose any additional weight after reaching 200 °C. The sample that was heated to 700 °C, showed an initial weight loss of ~2 % below sublimation temperature and only an insignificant 0.7 % loss above 400 °C and during a 20 h dwell time at 700 °C. Such small weight loss shows that only a negligible amount of V_2O_5 could be lost during heat treatments.

References

1. Rodriguez-Carvajal, J. FULLPROF: a program for Rietveld refinement and pattern matching analysis. in vol. 127 (Toulouse, France, 1990).

2. Rodriguez-Carvajal, J. Recent Advances in Magnetic Structure Determination by Neutron Powder Diffraction. *Phys. B Condens. Matter* **192**, 55–69 (1993).
3. Togo, A. & Tanaka, I. First principles phonon calculations in materials science. *Scr. Mater.* **108**, 1–5 (2015).
4. Togo, A., Oba, F. & Tanaka, I. First-principles calculations of the ferroelastic transition between rutile-type and $CaCl_2$-type SiO_2 at high pressures. *Phys. Rev. B* **78**, 134106 (2008).
5. Gonze, X., Charlier, J.-C., Allan, D. C. & Teter, M. P. Interatomic force constants from first principles: The case of α-quartz. *Phys. Rev. B* **50**, 13035–13038 (1994).
6. Gonze, X. & Lee, C. Dynamical matrices, Born effective charges, dielectric permittivity tensors, and interatomic force constants from density-functional perturbation theory. *Phys. Rev. B* **55**, 10355–10368 (1997).
7. Miliūtė, A. *et al.* Synthesis and phase purity of the negative thermal expansion material ZrV_2O_7. (2024) doi:10.5281/zenodo.12688634.